W. Schuhmann and A. Schulte

DOI: 10.1002/anie.200604851

Scanning Electrochemical Microscopy

Single-Cell Microelectrochemistry

*Albert Schulte and Wolfgang Schuhmann**

Keywords:
exocytosis · living cells · scanning electrochemical microscopy (SECM) · ultramicroelectrodes · voltammetry

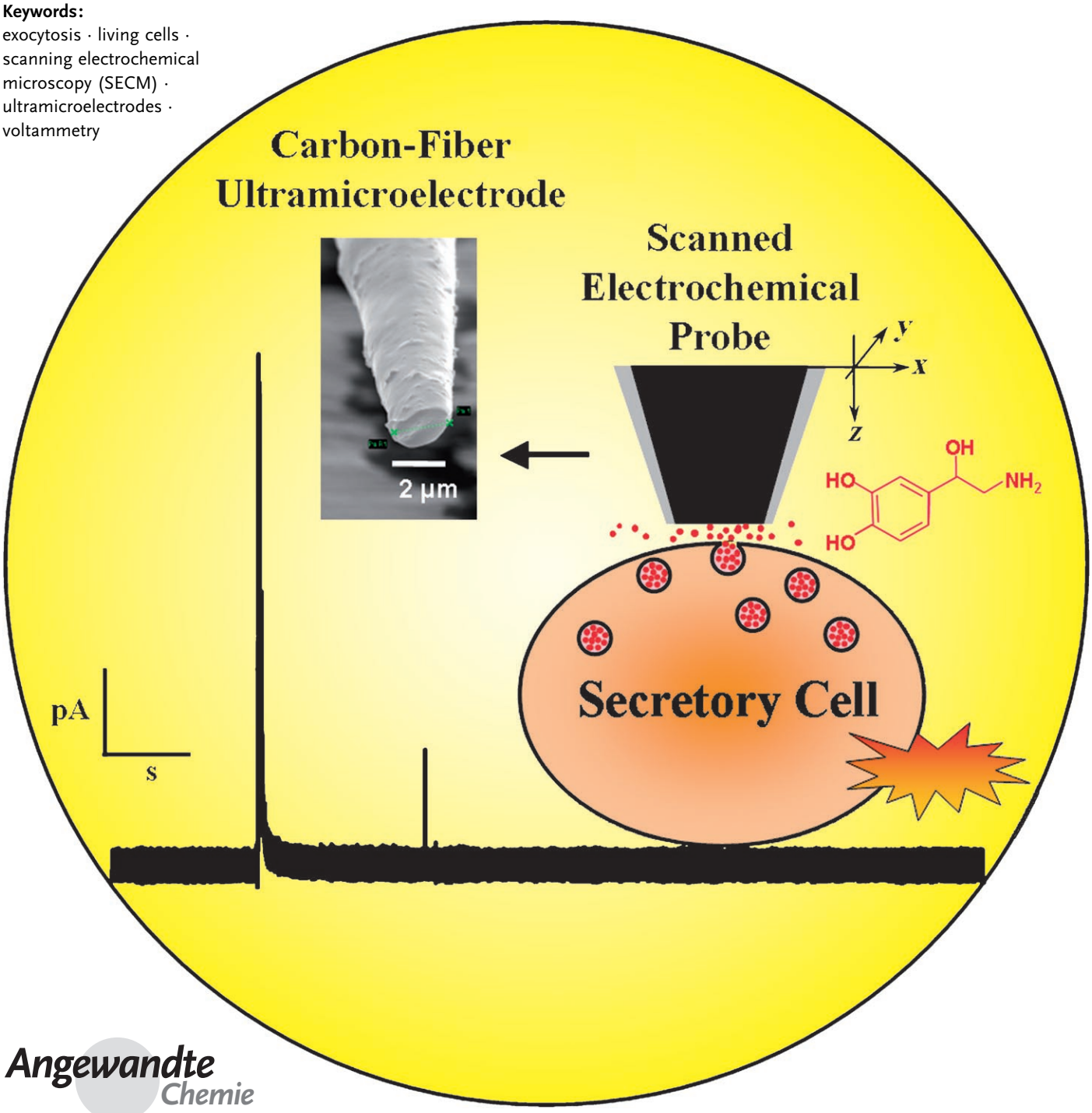

Needle-type voltammetric ultramicroelectrodes show exceptional sensitivity for the detection of redox-active substances, rapid response times, and total tip diameters in the lower micrometer range. These characteristics make them ideal for analyzing the chemical environment and the activity of isolated living cells, which in their various forms are the microscopic building blocks of human, animal, and other life forms. Prerequisites for successful local electrochemical measurements in the vicinity of the tiny biological objects are gentle, stress-free, and accurate placement of the tip at the cell, exact knowledge of the tip-to-cell distance, and appropriate selectivity of the ultramicroelectrode tip for species that may change in concentration as a result of cellular actions such as growth, respiration, or transmitter and metabolite uptake or release. The concepts of single-cell microelectrochemistry are considered and an overview is given of recent results on the fundamental mechanisms of cell functions.

From the Contents

1. Introduction

Vast technological improvements in the areas of integrated electronic circuits, microprocessors, and software in the past few decades have brought about major advances in electrochemical instrumentation. This progress allowed electrochemistry, already a well-established scientific field, to make remarkable steps forward in almost all its fields of application. Easy-to-use, high-precision computerized potentiostats appeared on the market and allowed the measurement of very small currents with superb noise levels and accuracy. In parallel, the routine fabrication and positioning of ultrasmall voltammetric electrodes in many laboratories enabled their use as miniaturized electroanalytical tools for the determination of redox-active compounds with high spatiotemporal resolution, excellent sensitivity, and low detection limits.

In voltammetry, a constant or systematically changing potential is applied to the working electrode and its current response is monitored as a function of time and/or potential. Unlike conventional electrodes, voltammetric ultramicroelectrodes (UMEs) have their characteristic geometric dimension (e.g. the diameter/radius for disk or the width for band electrodes) significantly decreased from the macroscopic to the microscopic scale.[1] The resulting extremely small active electrode surfaces, however, are intrinsically associated with very tiny measurable currents, and it was in fact the access to highly sensitive electrochemical amplifiers and the ability to precisely monitor current levels down to several 100 fA that paved the way for more broadly exploring the range of applications of voltammetric UMEs in trace analysis, kinetics measurements, as well as surface and biomedical sciences.

Voltammetric UMEs are now available with various geometries (cylinder, hemisphere, disk, band, ring, and combinations thereof), dimensions (μm to nm), and materials (C, Pt, Au, Ag). Their theory, fabrication, and performance have been presented in a monograph[2] and in several review articles.[3] Briefly, the advantages of UMEs for voltammetric and chronoamperometric experiments include:

1) improved signal-to-noise ratio primarily because the analytically relevant Faraday currents are greatly enhanced; this enhancement results from the hemispherical or spherical (rather than planar) diffusion towards UMEs, which produces higher mass transfer rates of the electroactive species;
2) less distortion of measurement by the iR drop, because the total currents (i) typically measured at UME working electrodes are smaller than those at conventional electrodes. Thus, measurements can be performed in highly resistive solutions (e.g., solutions without added supporting electrolyte);
3) a fast response time owing to the small double-layer capacitances (C) and thus low RC time constants (τ). This property allows rapid changes in the concentration of redox-active species to be monitored at nanosecond time scales;
4) the small overall size enables electrochemical experiments in limited volumes and at microscopically small objects.

With their outstanding electroanalytical and geometrical properties, needle-type UMEs with micrometer-sized total tip dimensions are superior for spatially and temporally resolved

[*] Prof. Dr. W. Schuhmann
Analytische Chemie—Elektroanalytik & Sensorik
Ruhr-Universität Bochum
Universitätsstrasse 150, 44780 Bochum (Germany)
Fax: (+49) 234-3214683
E-mail: wolfgang.schuhmann@rub.de
Assoc. Prof. Dr. A. Schulte
School of Chemistry, Institute of Science
Suranaree University of Technology
111 University Avenue, Muang District, Nakhon Ratchasima 30000 (Thailand)

voltammetric measurements in biological systems and hence intensely utilized in the life and medical sciences. The most active disciplines are neurochemistry and cell physiology, in which miniaturized voltammetric sensors are frequently employed for observing the dynamics of a variety of cellular processes and tracking changes in the chemical composition of the intra- and extracellular fluid. These changes are either attributable to cell activities such as growth, reproduction, respiration, and cell-to-cell communication, or they reveal metabolic reactions that result from strains and stresses such as food shortage, physical exercise, or drug uptake. In general, in vivo applications in which the active tips of UMEs are implanted with as little impact as possible into selected tissue of laboratory rodents must be distinguished from in vitro applications on isolated biological cells or acute tissue slices.

In vivo voltammetry in the central nervous system of living animals with the aim of elucidating the neurochemistry of cells involved in complex behavior is certainly one of the exciting applications of this type of electroanalysis. The field was actually established by Adams and co-workers at the beginning of the 1970s with their efforts to observe fluctuations in the levels of catecholamine neurotransmitters in various regions of the rat brain subsequent to stimulated synaptic release.[4] Since this pioneering work, the progress of in vivo voltammetry has been remarkable, which is reflected in the number of published review articles.[5] Two recent achievements are the wireless voltammetry in the brains of freely moving rats by implementation of telemetric systems[6] and the real-time monitoring of naturally occurring tonic or phased dopamine signals in the extracellular fluid of different regions of the brain of alert (not anesthetized) rats, which were correlated to behavior as diverse as sexual arousal, reward, food and novelty seeking, or drug-taking.[7,8]

This review article focuses on single-cell microelectrochemistry, or to be more exact electrochemical measurements that are performed with voltammetric UMEs on the smallest sustainable units of life—isolated biological cells in cell cultures. Although estranged from their indigenous surroundings, individual isolated or cultured cells can sustain their characteristic metabolic and (neuro)physiological processes, thus resembling to a certain extent cells in the body. Accordingly, single cells are good experimental model systems for examining complex biological processes and functions in a controlled and straightforward manner. In general, these experiments are not influenced by interferences that often cause problems in the highly heterogeneous intact tissue. However, living cells have microscopic dimensions, and responses attributable to their distinct activity are therefore small and often occur on a very fast timescale. Screening and visualizing of single cells hence require sophisticated analytical techniques with adequate sensitivity and high spatiotemporal resolution. Examples include advanced optical[9] and electrophysiology techniques,[10] and the use of voltammetric UMEs.

Figure 1 shows some cellular systems that can be studied by single-cell electrochemistry. The individual cultured living cells can be derived from (commercially) available cell lines or from primary cell cultures that are established from a fresh preparation of animal tissue. Genetically modified cells with specific defects can be obtained by well-established procedures of cell transfection applied to cultured mother cells or by using cell preparations from genetically engineered animal mutants (e.g. knockout mice or rats). Through comparison with their "wild-type" analogues, transfected and transgenic cells provide models for studying gene functions or complex actions such as vesicular transmitter or hormone release. The role of a (knocked-out) gene or of the associated proteins in particular processes can thus be evaluated.

In general, voltammetric detection can be performed with either positionable, needle-like UMEs (Figure 2) or with UME arrays consisting of many individually addressable voltammetric sensing entities. The arrays can be produced by nano- and microdevice manufacturing technology,[11] in particular, adapted silicon fabrication processes, and, in contrast to tapered sensor tips, do not require highly accurate positioning techniques. Instead, the cells to be studied are cultured (seeded) on top of the microelectrode assembly, where cellular processes such as the release or consumption of electroactive substances are then assessable by various voltammetric detection methods. Depending on the size of the individual active elements of UME arrays relative to the size of single cells and the space between discrete microelectrode surfaces, information can be acquired either from various spots on one cell or from multiple cells. The detection of catecholamine exocytosis from secretory cells,[12] as well as neuronal transmitter[13] and nitric oxide (NO) release[14] on chiplike devices are examples of studies of the activity of single cells with UME arrays. The multiple test sites available

Albert Schulte received his PhD in 1994 from the University of Münster (Germany). After postdoctoral research at the Max Planck Institute for Experimental Medicine in Göttingen (Germany) and at the University of Edinburgh (Scotland), he joined Wolfgang Schuhmann's group at the University of Bochum (Germany) as a Senior Research Officer. In January 2006, he became Senior Lecturer in Physical Chemistry at the University of the West Indies in Trinidad and Tobago, and in April 2007 joined the faculty of Suranaree University of Technology in Nakhon Ratchasima (Thailand), where work is directed towards various aspects of micro-, nano-, and bioelectrochemistry.

Wolfgang Schuhmann obtained his PhD in 1986 at the Technical University of Munich (Germany). After finishing his habilitation thesis there in 1993, he was appointed to Professor for Analytical Chemistry at the University of Bochum in 1996. His research interest addresses the development of reagentless amperometric biosensors, microelectrochemistry, the miniaturization of biosensors, scanning electrochemical microscopy, electrochemical robotics, miniaturized sensors for local measurements at biological cells, localized corrosion, and microelectrochemical investigations of fuel-cell catalysts.

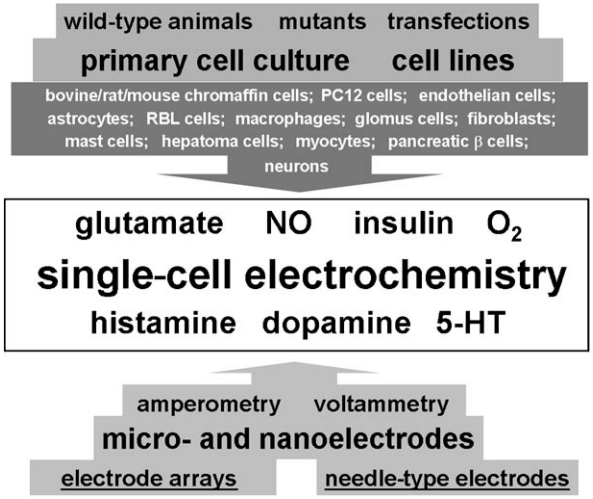

Figure 1. Representative systems that have been studied by single-cell microelectrochemistry. Top: Individual living cells can be obtained either through enzymatic dissociation of explanted tissue of laboratory rodents or farm animals or from the many commercially available cell lines and may be genetically modified for specific cell activity measurements. Bottom: Single cultured cells may be studied with the tips of pointed micro- or nanoelectrodes positioned close to their plasma membranes or while resting on the active microscopic surfaces of microelectrode arrays. For the detection of electroactive species in the vicinity of active cells, the chosen microsensors may be operated in a voltammetric mode by continuously changing the working electrode potential E as a linear function of time t between two user-defined values with $\Delta E/\Delta t$ referred to as the scan rate or in an amperometric mode by keeping E at a constant value that is appropriate to oxidize or reduce the redox species of interest.

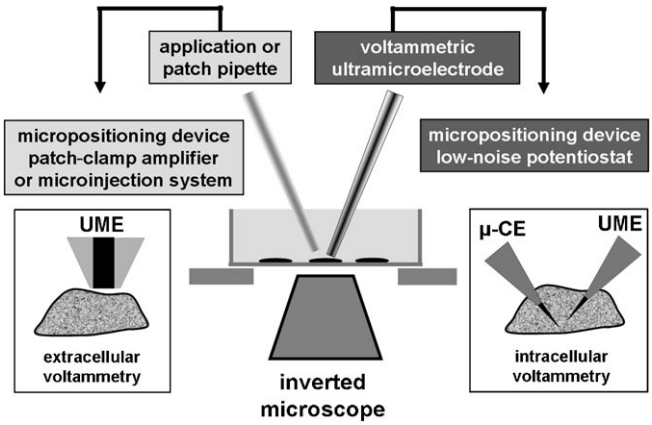

Figure 2. Schematic of an electrophysiological workstation for electrochemical single-cell experiments with needle-type voltammetric microelectrodes. An inverted microscope is used to operate an application or patch pipette for cell stimulation and the voltammetric ultramicroelectrode (UME) for electrochemical detection of cellular responses. Both tools must be attached to precise micropositioning devices for careful placement of their tips next to (extracellular voltammetry) or inside (intracellular voltammetry) a single living cell. The utilization of low-noise electrochemical amplifiers with the ability to monitor currents in the fA to pA range guarantees the sensitivity needed for tracing tiny changes in concentration of redox-active species resulting from cellular activities such as secretion or respiration. μ-CE: needle-type micro-counter electrode.

on striplike sensor devices and the suitability for automated loading and analysis make UME arrays suitable for high-throughput screening of cellular activity. Several analytes can be detected simultaneously and interconnected networks of neuronal or other cells can be chemically probed. However, the possible applications of UME arrays in voltammetric detection at the single-cell level have not yet been fully explored.

The first section of this review gives a general overview of methods for the fabrication of voltammetric UMEs with tips that are appropriate for in vitro voltammetric measurements inside the cytoplasm (intracellular voltammetry) or in close proximity of single biological cells (extracellular voltammetry). Selected examples of reports on intracellular voltammetry and on conventional "extracellular" voltammetric detection of chemical messengers such as catecholamines, nitric oxide (NO), and glutamate, monitored with stationary UME tips placed next to the outer membrane of a secretory cell are briefly discussed. Scanning electrochemical microscopy (SECM), a scanning probe microscopy technique that uses precisely movable voltammetric or potentiometric UMEs as high-resolution imaging tools, has been established[15] and applied for single-cell studies in which cell morphology and cellular (redox) activity are imaged simultaneously.[16] Theoretical and practical aspects that are relevant for SECM measurements on living cells are provided. This section includes a discussion of the drawbacks of the constant-height mode and the advantages of the constant-distance mode of SECM for imaging soft three-dimensional biological objects. Important developments in SECM instrumentation are reviewed and illustrations of single-cell SECM studies are used to highlight the impact that single-cell SECM may have as a modern electrochemical tool in different disciplines of life science and medicine. Finally, potential future aspects and challenges of single-cell electrochemistry are discussed.

2. Voltammetric UMEs for Detection at and in Single Living Cells

Quite a few papers over the past years have described procedures for the fabrication of tiny voltammetric probes that are, in addition to other microelectrochemical applications, suitable for spatially confined measurements very close to or even inside living cells. The optimum type of electrode is very much dependent on the particular cell and the cellular process under investigation. In any case, voltammetric UMEs for single-cell electrochemistry should offer not only an appropriate tip size but also excellent sensitivity towards the analyte, low background current, and good stability in physiological buffer solutions. Furthermore, they should be easy to fabricate and handle. The materials used predominantly for the fabrication of UMEs are carbon and platinum. Carbon is ideal for detecting the release of catecholamine neurotransmitters in physiological saline solutions, as carbon electrode surfaces are less susceptible to electrode fouling. Platinum is favored for measuring, for example, extra- or intracellular concentrations of oxygen thanks to its electrocatalytical properties.

For single-cell measurements in the extracellular space very close to single living cells, the preferable sensor geometry is a disk or disklike active electrode surface, a nonbulky insulation in the apex region, and dimensions not bigger than that of the investigated cells themselves. The electrodes can be fabricated by sealing carbon fibers with graphite-like conductivity or Pt microwires with diameters down to about 5 μm in glass or polymer coatings, thus exposing electroactive microdisks surrounded by an insulating sheath after careful polishing (glass) or scalpel transection (polymer). Three types of low-noise carbon-fiber ultramicroelectrodes (CF-UMEs) with typical diameters of the carbon disks of about 5–10 μm are routinely used for neurotransmitter release measurements on secretory cells and individual cultured neurons:

1) "Wightman-type" glass-insulated CF-UMEs with elliptical geometry,[17]
(2)"Chow-type" polyethylene (PE) or -propylene (PP) insulated disk-shaped CF-UMEs,[18] and
3) "Schulte-type" electropainted disk-shaped CF-UMEs.[19]

Glass-insulated CF-UMEs are fabricated by sealing single carbon fibers with epoxy glue tightly into fine tips of pulled glass capillaries and then cautiously polishing the tip at a 45° angle on a micropipette beveller to produce an oval surface. The electroactive area of the polished carbon microellipse is more than twice that of a disk electrode from the same material. At the same time, the background current is not significantly increased,[17] so the sensitivity is improved. PE- or PP-insulated CF-UMEs are obtained by loading short pieces of thin PE or PP tubes with single carbon fibers and then locally melting and pulling them. In this way, the carbon fiber is trapped within the tip of a tapered plastic pipette and covered with an almost invisible thin polymer film. Cutting the plastic tip under a microscope with sharp razor blades finally reveals the required carbon microdisk. The production of PE- or PP-insulated CF-UMEs is, however, fiddly.

Comparatively simple is the fabrication of disk-shaped CF-UMEs that are insulated by means of electrodeposition of paint. This procedure is used in the canning and automobile industry for effectively providing chemically stable anticorrosion coatings. Water-based electrodeposition paints (EDPs) are commercially available as anodic and cathodic systems. Their electrochemically induced deposition onto conducting surfaces is based on the pH-dependent solubility of the applied polymers. For example, an anodic EDP is made up of an aqueous dispersion of "water-soluble", negatively charged micelles of a poly(acryliccarboxylic acid) resin. The target to be electropainted forms the anode in an electrochemical cell, which contains the EDP suspension as electrolyte and is kept at a potential that is suitable for vigorously splitting water by anodic oxidation to generate protons at the anode/electrolyte interface. Negatively charged EDP micelles migrate towards the oppositely charged anode, where the acidification of the electrolyte near the electrode surface protonates the carboxylate side groups of the polymer and lowers their solubility. This well-controlled process results in the deposition of a film of EDP paint on the entire immersed electroactive surface. The precipitation of an EDP leads to even, thin, and defect-free layers on carbon fibers that bind tightly to the carbon surface. To transform the water-containing polymer film into a well-insulating dielectric that resists decomposition even at high voltages and insulates the cylindrical face of the fiber, the freshly electropainted carbon fiber must be cured at elevated temperature. Immediately before use, the tip is cut with a scalpel to give a thinly insulated carbon microdisk (Figure 3).

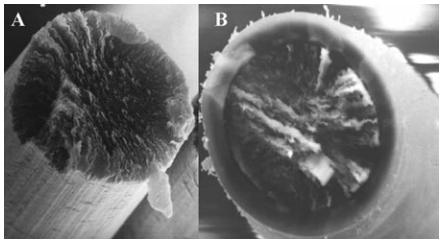

Figure 3. Scanning electron microscope (SEM) images of the endings of 10-μm-diameter carbon fibers covered without (A) and with (B) a thin layer of an electrodeposition paint (EDP paint) covering the cylindrical but not the disk face of the carbon filament. The disk-shaped face of the carbon filament has been exposed by careful transection with a sharp scalpel blade to form the active tip of the carbon-fiber ultramicroelectrode (CF-UME), as typically used for neurotransmitter and hormone release measurements on single secretory cells.

Carbon disk UMEs with even smaller diameters are required for improved spatial resolution in the local detection of cellular catecholamine transmitter release. However, the precursors for disk-shaped CF-UMEs, high-performance carbon fibers, are normally used as structural components in fiber-reinforced plastics and are commercially available only with diameters down to about 5 μm. Thinner carbon fibers for ultrasmall (disk-shaped) CF-UMEs could be obtained by electrochemical,[20] electrical,[21] flame,[20c,22] or ion beam[23] etching procedures for tapering carbon fibers. CF-UMEs with effective radii of less than 1 μm could be prepared by further subjecting conically or cylindrically etched carbon fiber tips to an applicable insulating strategy, such as electrochemically induced polymer deposition.[20a,22c,24] In another approach, very small carbon disk UMEs were fabricated by pyrolysis of short-chain alkanes on the inside walls of the tips of heated quartz micropipettes. The pipette openings were completely filled with carboneous material. The obtained deposit showed sufficient conductivity to be used as miniaturized electrode surface.[25]

The detection of chemical messengers other than catecholamines at the single-cell level relies on the use of chemically modified UMEs with catalytic activity towards redox reactions of the analyte of interest. Information on modification strategies used to optimize the detection of physiologically important molecules such as NO, glucose, or insulin in biological samples can be found in recent review articles.[26] Surface modification with porphyrin complexes was shown to be optimal to produce UMEs for the detection of NO release from single cells. Miniaturized enzyme-based microbiosensors incorporating glucose (GOx) or glutamate (GluOx) oxidase have become tools for single-cell glucose and glutamate monitoring. Single-cell insulin secretion could

be detected at disk-shaped UMEs covered with mixed-valent ruthenium oxide/cyanoruthenate films.

Bare, disk-shaped Pt UMEs are predominantly used for local measurements of O_2 in the extracellular milieu adjacent to "breathing" living cells. Typically, they are made by sealing Pt microwires in thin tapers of pulled glass capillaries and then polishing to produce glass-sealed Pt tips. Various miniaturized, membrane-covered Clark-type O_2 electrodes for single-cell studies are commercially available. Nanometer-sized Pt UMEs[27] have recently been described by several groups. These UMEs could be suitable for improving the spatial resolution of the detection of cellular O_2 consumption. However, the potential for this application has not yet been explored because of the difficulties in their accurate positioning at the cell membrane. A self-referencing, polarographic, O_2-selective microelectrode was developed for measuring O_2 fluxes from single cells with a good sensitivity and spatial resolution in real time.[28]

Disk-shaped electrodes are well-suited for extracellular measurements, but intracellular voltammetric detection requires much sharper UMEs. The tips must be able to smoothly penetrate cell membranes to reach the cytoplasm without serious cell damage. Already in 1967, the design of a voltammetric microelectrode for measuring intracellular partial pressure of O_2 was reported.[29] Much later, Ewing's group constructed ultrasmall carbon ring UMEs,[30] which could be used for intracellular voltammetry of dopamine[31] and, upon surface modification with layers of Pt/nafion or Pt/GOx/nafion, of O_2[32] or glucose,[33] respectively. Meulemans et al. developed methods for the construction of needle-type, glass-insulated Pt[34] and C[35] microelectrodes for intracellular voltammetric measurements of redox-active species. Taha and co-workers reported already in the early 1990s that chemically modified tips of flame-etched and polymer-insulated carbon fibers can be effectively pushed through cell membranes and used in the cytoplasm for quantifying trace levels of NO[36] (CF-UME coated with thin polymeric films of TMHPP-Ni/nafion; TMHPP-Ni = nickel(II) tetrakis(3-methoxy-4-hydroxyphenyl)porphyrin) and metal ions[37] (CF-UME coated with TMHPP-Ni/nafion or mercury).

3. Examples of Intracellular Voltammetry

The meta- and catabolic pathways that are responsible for an ongoing biochemical processing and signaling within the cell cytosol naturally engage a vast number of (bio)chemical compounds, some of which carry redox-active functionalities and hence are voltammetrically detectable. The development of intracellular voltammetry was thus motivated by the desire to track in real time the dynamics of cytosolic metabolites and chemical transmitter molecules, including time-dependent changes in their concentration as result of membrane trafficking. Such knowledge is important for a better understanding of the behavior of individual cells in terms of their metabolism, function, and regulation. Additionally, the investigations may help to reveal the signaling mechanisms that are employed by large networks of cells for intercellular communication. Furthermore, quantitative detection of the transport of electroactive drugs and toxins across cell membranes may provide helpful information for developments in pharmacology and toxicology.

In the 1980s, a number of laboratories developed voltammetric probe tips that were sharp enough to pierce cell membranes with minimal damage and negligible loss of sensitivity. The first reports explored the potential of microelectrode voltammetry in the interior of cells for monitoring intracellular concentrations of O_2, glucose, NO, and a number of biologically relevant trace metals and drugs. Meulemans et al., for example, exposed individual cultured neurons from the dissected buccal ganglions of the marine mollusk *Aplysia Californica* to physiological buffer solutions with or without antipyrine and metronidazole. They then followed the time course of the cellular uptake and clearance of these redox-active drugs by means of intracellular differential pulse voltammetry (DPV).[35] They could also determine the intraneuronal concentration of serotonin (5-HT) in live serotonergic metacerebral cells of the same animal. Changes in intracellular 5-HT concentrations were measured in real time with DPV at needle-type, glass-insulated Pt UMEs for several hours after neuronal stimulation, intracellular injection of 5-HT, or extracellular application of L-tryptophan, reserpine, or *p*-chlorophenylalanine.[34] Tips of carbon-ring UMEs were placed inside the giant dopamine neuron of the snail *P. Corneus* and operated in amperometric mode at constant anodic potential to monitor cytosolic concentrations of dopamine and to quantify its membrane transport and metabolic clearance.[31,38] These investigations proved that the refilling of freshly formed but still empty intracellular storage vesicles with locally available messenger molecules is an important process at the early stage of exocytosis but has to compete efficiently with the escape of the transmitter through the cell membrane.

Respiration is an additional activity that is of critical importance for the proper physiological function of single cells. Efficient O_2 uptake is strongly related to sufficient provision of energy for the various biochemical processes in the cytoplasm. Ewing et al. used intracellular quantitative O_2 monitoring at nafion-coated platinized carbon-ring UMEs for accessing the relative cytosolic O_2 concentrations of giant dopamine neurons of *P. Corneus* (another preparation routinely used in single-cell neuroscience experiments). Comparison of the values obtained from resting neurons and neurons stimulated by high potassium concentration suggested that increased intracellular O_2 consumption took place upon evoked vesicular dopamine release. This effect was related to an increase in internal energy consumption of the cells for vesicle transport and exocytosis.[32]

Gaseous NO may act in biological systems as a cytotoxic agent or as a fast-diffusing molecular messenger. NO is able to quickly mediate a variety of signaling pathways in the target cells and as such is known to be involved in processes such as neuronal signaling, immune response, modulation of ion channels, cellular defense mechanisms, and vasodilatation. NO is synthesized within particular cells through the Ca^{2+}/calmodulin-dependent enzymatic reaction of NO synthase (NOS) with conversion of L-arginine to citrulline. Thus, a detailed investigation of the complex mechanisms behind an

NO-regulated cellular function involves the elucidation of the dynamics of intracellular NO production. Malinski and Taha were the first to attempt this task electrochemically by placing the tips of NO-sensitive CF-UMEs inside individual cultured endothelial cells. The sensors were applied in real time for voltammetric monitoring of the increase in cytosolic NO levels that occurs following bradykinin-stimulated onset of NOS activity.[36] If poly-TMHPP-Ni films on CF-UMEs were subjected to demetalation in acidic solutions, the sensor was able to reincorporate Ni^{2+} ions very selectively by means of an ion-exchange process in which protons from the porphyrin rings are exchanged for Ni^{2+} ions. The current from the Ni^{2+}/Ni^{3+} oxidation in the polymeric film generated the analytical signal for Ni^{2+} ion quantification. This strategy, employed in the cytosol of individual myocytes and hepatoma cells, was sensitive enough to detect low concentrations of Ni^{2+} ions in cells and follow the time course of Ni^{2+} ion uptake in the cytoplasm when the cells were incubated in buffer solutions containing higher concentrations of this ion.[37]

The above-mentioned examples show that intracellular voltammetry can provide insights into physiologically relevant cellular activities. However, in contrast to investigations by extracellular voltammetry at disk-shaped UMEs near the outer of cells, the initial phase of enthusiasm was followed by a significant drop in research activity, which may reflect at least to a certain extent the difficulty in fabricating good-functioning probe tips for intracellular electrochemical measurements and placing and operating them at the right place without too much harm to the living objects of study.

4. Examples of "Conventional" Extracellular Voltammetry

"Conventional" extracellular voltammetry is defined herein as voltammetric detection carried out with disk-shaped UMEs that are brought into extreme proximity to the outer cell membrane with the aid of an inverted microscope and user-controlled motorized, piezoelectric or hydraulic micropositioning devices but not supported by any topographic information about the investigated cell.

The most prominent example of this type of biological voltammetry is the highly sensitive electrochemical detection of Ca^{2+}-dependent regulated exocytosis, a well-synchronized cascade of intracellular events (Figure 4A) executed by secretory and neuronal cells for the release of hormones and neurotransmitters from membrane-bound cytosolic storage vesicles into the extracellular space or synaptic cleft. In steps that precede exocytosis, secretory vesicles are formed and loaded with a particular chemical transmitter. The packed vesicles are initially kept in a reserve pool and, when needed for cell signaling, transported towards the plasma membrane, with which they tether and dock upon arrival by complex interactions between their membrane proteins. A newly docked vesicle has to go through a series of molecular rearrangements of the established protein bonds before it is ready for instantaneous release. A suitable external stimulus able to trigger the opening of Ca^{2+} ion channels will at this stage almost instantaneously induce exocytosis through the sudden increase in intracellular Ca^{2+} ion concentration. Fusion of the vesicular and plasma membranes will occur and be followed by the opening of a tiny fusion pore and complete discharge of transmitter molecules from the lumen of the collapsing vesicle.

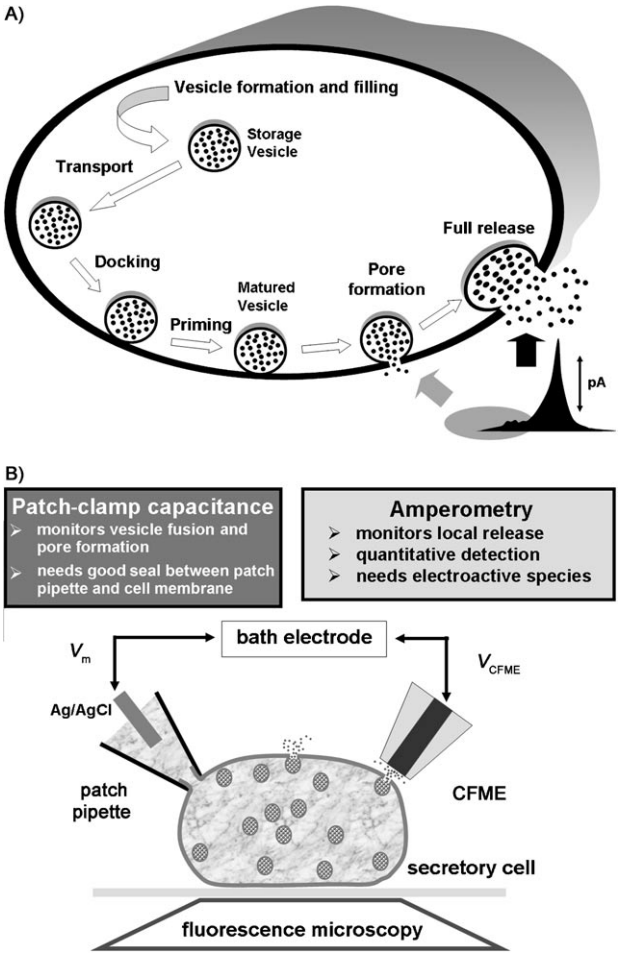

Figure 4. A) The steps involved in Ca^{2+}-triggered secretory vesicle exocytosis leading to quantal release of secretory products. Amperometric current spikes resulting from oxidation of discharged transmitter molecules at a close CF-UME reveal the late steps of the fusion pore opening as a smaller preceding "foot signal" and full release as a more pronounced boost. B) The three main analytical approaches for following intracellular movements of secretory granules and monitoring exocytotic release of neurotransmitters and hormones in real time and on the level of single fusing and releasing secretory vesicles: *Fluorescence microscopy* in its various configurations can visualize the entire life cycle of a secretory vesicle when its content and/or membrane are labeled with powerful fluorescent dyes. *Patch-clamp capacitance measurements* are able to monitor changes in total capacitance of the cell membrane and thus detect the processes of fusion of vesicles and opening of fusion pores. *Amperometry* at suitably placed, polarized carbon-fiber ultramicroelectrodes can detect with excellent sensitivity the oxidation of chemical messenger molecules at the sensor tip and provides information about the time course of the release event.

A well-ordered dynamic interaction of the many vesicle and plasma membrane proteins was found to be of key importance not only for vesicle docking and maturation but also for the later timing of membrane fusion and release of

secretory products.[39] The exact function of the identified proteins and their impact on the dynamics of vesicle exocytosis thus became a very active area of research with the goal of unraveling the molecular mechanisms behind this common mode of chemical cell-to-cell signaling in the human brain and the mammalian nervous system.

Figure 4B depicts three modern bioanalytical detection schemes that are frequently used for studying the distinct phases of vesicular release of chemical messengers at the level of single cells. Sophisticated variants of high-resolution fluorescence microscopy have been developed into routine optical tools for the detailed investigation of practically every step throughout the life cycle of secretory vesicles. The success of the method relies strongly on the choice of a suitable fluorescent label for the reactants and the quality of sensitive optical imaging techniques, such as confocal and total internal reflection microscopy.[40] The progress of membrane fusion and fusion pore opening at the beginning of single-vesicle exocytosis has also been revealed by means of high-resolution patch-clamp cell-membrane capacitance measurements.[41] The technique is actually sensitive enough for visualizing in real time the tiny increases in cell surface area resulting from the incorporation of the membrane of fusing granules as noticeable differences in the total membrane capacitance. Finally, spatially confined voltammetry at CF-UMEs positioned close to the cell membrane is a complementary indicator of fusion events. It provides a highly sensitive, direct, and quantitative measure of both the early leakage of transmitter molecules out of premature fusion pores and the complete release from the finally fully collapsed secretory vesicles. The advantages and limitations of constant-potential carbon-fiber amperometry and carbon-fiber fast-scan cyclic voltammetry as well as applications of these methods for the detection of exocytosis from single cells and a description of the analysis of data from such measurements are covered in several review articles.[42]

The adrenal glands of cows and rats provided the first model secretory cells at which direct electrochemical detection of distinct exocytotic events was achieved.[43] In the pioneering trials, the tip of an anodically polarized disk-shaped CF-UME was placed as close as possible to the cell membrane of an individual adrenaline-releasing chromaffin cell and the low-noise amperometric current response of the microelectrode was monitored over time. Under these conditions, chemical cell stimulation led reproducibly to the appearance of bursts of current spikes, which could be related to the release of discrete packets ("quantums") of neurotransmitter molecules from single fusing and collapsing vesicles. The released neurotransmitter molecules were detected by electrochemically induced oxidation of the secreted species at the ultramicroelectrode surface. After the initial experimental breakthrough, amperometric detection of secretion was further improved and soon demonstrated to be capable of detecting even the small pedestal or "foot" signals that occasionally occur at the onset of unitary exocytotic current spikes. These pedestal signals correspond to slow leakage of catecholamine molecules out of just-opened narrow fusion pores prior to complete vesicle collapse and exocytosis.[44]

It was recognized quickly that quantitative analysis of the characteristic features of the current transients in amperometric recordings of exocytosis events could offer valuable information about the mechanism and kinetics of exocytotic neurotransmission. The obligatory secretory spike analysis and interpretation has to be a thorough statistical treatment of key parameters such as the spike frequency, rise time, amplitude, charge, and half-width as well as the number and contours of the foot signals. As amperometric recordings of single-vesicle exocytosis usually involve huge data files, user-written acquisition/analysis software in different programming languages has been developed for manual or automatic spike analysis.[44,45] On average, a certain number of transmitter molecules are released from each vesicle. Thus, the presence of a population of vesicles varying in size or concentration of their content can be derived from histograms of the charge transferred during individual spikes. The time course of the fusion pore opening and the late period of the release may be assessed by interpreting the distribution of the rise times and half widths of the spikes. If the chemical nature of the released transmitter is unknown, it can be determined by fast-scan cyclic voltammetry at the positioned CF-UME;[46] the background-subtracted voltammograms act as fingerprints for identification of the secretory products. Voltammetric detection of exocytosis can normally be performed only on cells that secrete readily oxidizable neurotransmitters or hormones. To circumvent this limitation, cell culture protocols have been developed for loading secretory cells with exogenous neurotransmitters that are readily oxidized on a suitably polarized CF-UME.[47]

On its own or in conjunction with patch-clamp and fluorescence measurements, single-cell carbon-fiber amperometry is today a standard microelectrochemical assay for investigating the molecular events that mediate the exocytotic release of chemical messengers. Isolated bovine, rat, or mouse chromaffin cells have been systematically studied and are still under thorough investigation as native or genetically modified preparations.[48] Other cells used in exocytosis research include pheochromocytoma (PC12) cells,[49] mast cells,[49d,50] pancreatic beta cells,[49d,51] human carcinoid BON cells,[52] rat basophilic leukemia (RBL-2H3) cells,[53] rat hippocampal astrocytes,[54] various cultured neurons,[55] chromaffin cells (for example, in slices of mouse adrenal glands),[56] glomus cells in slices of the rat carotid body,[57] and neurons in acute brain slices.[58]

The results of the many published studies—from which only a representative sample is cited in references [48–58]—have led to an improved understanding of how secretory cells from the endocrine systems and neurons from the brain release their chemical messengers. As reviewed recently in a number of publications, at least three different types of vesicular exocytosis have been identified.[39] According to an "all-or-nothing" mechanism, secretory vesicles fuse with the cell membrane, form a fusion pore, collapse, and distribute their entire contents straight into the extracellular milieu. However, after formation the narrow fusion pore sometimes fluctuates around a small mean pore diameter ("fusion pore flickering") or even closes again transiently, before finally expanding irreversibly and releasing its load. This flickering

mechanism is typical for the small synaptic vesicles of neuronal cells and may provide them with an option for controlling the level of release. A "kiss-and-run" mechanism was observed as a third type of exocytosis, whereby the vesicle briefly fuses with the plasma membrane, ejects a little of stored transmitter molecules, and then moves back into the cell, where it either may be used again for another run or first be refilled.

The fine details of fusion pore formation and dynamics are still poorly understood at the molecular level. Also, it is not yet known why neuronal cells and vesicles trigger a particular type of exocytosis under certain conditions. Achieving these goals requires continuation of systematic studies on genetically modified secretory cells that lack one of the many highly specialized secretory plasma and vesicle membrane proteins. Ideal experiments are multidimensional in terms of assessing the exocytotic response of targeted cells simultaneously with carbon-fiber amperometry and the complementary optical and electrophysiological detection schemes mentioned above. This level of detailed analysis of single-vesicle exocytosis should eventually allow the influence of individual proteins on pore formation and dilation as well as the time course of release to be resolved and help unravel how vesicular chemical release is orchestrated.

Some promising new electrochemistry strategies at the level of single secretory cells are worth being mentioned even though they are beyond our earlier definition of conventional extracellular voltammetry. For example, glass slides were patterned with optically transparent and electrically conductive indium tin oxide (ITO) to fabricate well-defined ITO microelectrodes onto which secretory cells can be seeded at a desired density for secretion experiments.[59] The suitability of the miniaturized ITO structures for combined optical and electrochemical studies on the single cell level has been demonstrated by Amatore et al., who were in fact able to apply the methodology for both imaging stained chromaffin cells with fluorescence microscopy and detecting their chemical release with the ITO microelectrodes operated as amperometric sensors.[59a] After further miniaturization and optimization, ITO-based microdevices could soon become tools for high-throughput optoelectrochemical screening of exocytosis. A microfluidic device for on-chip cell transport, cell location, and amperometric detection of single-cell secretion[60] and disk-shaped Pt-UMEs microfabricated at the bottom of an array of picoliter wells into which single chromaffin cells can be captured[61] have also been proposed for rapid and automated analysis of single-cell exocytosis. Hafez et al. microfabricated an arrangement of four closely spaced Pt microelectrodes on glass coverslips and used the device for the spatially defined detection of fusion pore openings at different release sites of a single secretory cell that was resting on top of the detector array and stimulated to release its transmitter.[12] Finally, cell-attached patch amperometry combining patch-clamp measurements of cell membrane capacitance changes (indicating vesicle size) with amperometry at a CF-UME that is placed inside of the patch pipette (quantifying transmitter release) was introduced in particular for studying the exocytosis of the smallest secretory organelle, the small synaptic vesicles.[62] These vesicles have diameters of only a few tens of nanometers, which is a lot smaller than the dense-core vesicles of chromaffin or mast cells; however, patch amperometry was sensitive enough to resolve in real time the modest capacitance changes induced by the fusion of synaptic vesicles and display them together with the corresponding amperometric spikes resulting from the actual release of the tiny amounts of vesicular transmitter.

The majority of current work on microelectrode voltammetry with UMEs positioned at the outer surface of single cells involves detection of the release of neurotransmitters and hormones (exocytosis) from secretory cells. This type of measurement was thus given the main emphasis herein; however, other important physiological processes can also be approached in a similar fashion. Good examples are: 1) the detection of transmembrane fluxes of oxygen with self-referencing oxygen-sensitive Pt microelectrodes,[28] 2) the electrochemical visualization of oxygen production in single algal protoplasts upon exposure to light,[63] 3) monitoring the cellular release of reactive oxygen species (e.g. the superoxide ion $O_2^{\bullet -}$, H_2O_2, or NO) in real time at microelectrodes placed next to the specific cells,[64] 4) the electrochemical detection of drug efflux from preloaded single cells with disk-shaped CF-UMEs,[65] and 5) the detection of cholesterol contained in the plasma membrane of single cells with Pt-UMEs modified with lipid membranes containing cholesterol oxidase.[66]

5. Single-Cell Scanning Electrochemical Microscopy (SECM)

The invention of scanning electrochemical microscopy (SECM) in the late 1980s marked a crucial event in interfacial science. SECM is based on the experimental observation of a remarkable phenomenon: the dependence of the small current through a disk-shaped UME induced by the conversion of a dissolved redox species at constant tip potential on the tip-to-sample separation L and the chemical nature of the solid/liquid interface.[15] The methodology of SECM and the state of the art of SECM instrumentation together with a wide range of biological and nonbiological applications have been summarized in a monograph[67] and a number of review articles.[68] The following section provides a brief description of the basic principles of the technique and reviews applications of SECM for measurements on the level of single cells.

5.1. Principles of SECM Imaging

When disk-shaped UMEs are positioned in the bulk of a solution containing a reversible redox species, they display a typical sigmoidal cyclic voltammogram and diffusion-controlled steady-state currents I_∞, at least at potentials that significantly exceed the redox potential of the mediator (Figure 5A). From the microelectrode diameter d, the diffusion coefficient D, and concentration c of the involved mediator, as well as the number of electrons n transferred in the redox reaction at the tip, I_∞ can be calculated as $2nFDcd$. If the UME is attached to a precise micropositioning device

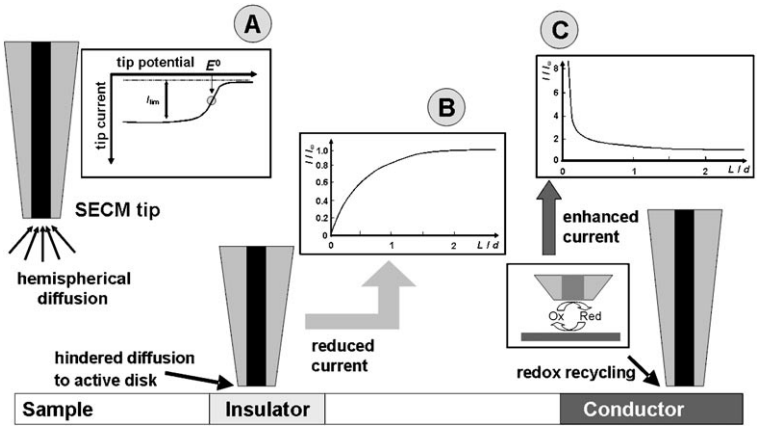

Figure 5. Principles of scanning electrochemical microscopy (SECM). A) In solutions containing a supporting electrolyte and, for example, a reducible redox-active compound, cyclic voltammetry at a disk-shaped ultramicroelectrode (UME, SECM tip) gives sigmoidal current/voltage curves with a steady-state, diffusion-limited current I_∞ measured at electrode potentials more cathodic than the redox potential of the dissolved redox mediator under the given experimental conditions. B,C) In *z*-approach curves, the amperometric tip current *I*, normalized with I_∞, is plotted as a function of the tip-to-sample distance *L*, normalized with the diameter of the UME *d*. The plots show the development of the tip current with decreasing distance to an electrochemically passive (insulating) or active (conducting) surface. B) In close proximity to an insulator, diffusion of redox-active species toward the electrode tip is physically hindered, which leads to a significant drop in the tip current *I* (negative feedback). C) Close to a conducting surface, redox species consumed at the tip can be recycled to their original oxidation state. With decreasing tip-to-sample distance *L*, recycling becomes more effective and the tip-current *I* increases (positive feedback).

and gently brought as an electrochemical scanning probe ("SECM tip") into close vicinity of an insulating specimen, the hemispherical diffusion of mediator molecules towards the active microelectrode disk is physically hindered and a drop in the tip current is observed (negative feedback, Figure 5B). In contrast, mediator molecules that were initially reduced (or oxidized) at the tip can be reconverted into their original state when the SECM tip is positioned above an electrochemically active surface. This redox recycling in turn leads to increased tip currents relative to those seen in the bulk solution (positive feedback, Figure 5C).

SECM imaging in the amperometric feedback modus takes advantage of surface-dependent modulation of the current signal and involves 1) operation of the SECM tip at a constant potential to obtain a steady-state current in the bulk solution, 2) approach of the SECM tip towards the sample surface and placement of the tip into the regime of either positive or negative feedback, and 3) a rastering movement of the probe tip at constant height *z* ("working distance") across the surface and measurement of the tip current as a function of lateral position (*x*,*y*). The optimal working distance for a given SECM tip can be determined by z-approach curves, which are plots of normalized tip currents (I/I_∞) versus normalized tip-to-sample separations (L/d). Changes in SECM tip currents obtained in constant-height (*x*,*y*) scans over homogeneously insulating or conducting surfaces reveal the surface topography (Figure 6). Current variations in feedback-mode SECM images of reasonable flat surfaces with neighboring conductive and insulating regions are indicators of the local changes in interfacial conductivity. However, no clear correlation can be obtained for rough samples that also exhibit a varying conductivity profile. The current at the SECM tip is a combination of the individual contributions of distance and local electrochemical activity of the surface, and hence additional information on the sample morphology is needed for a meaningful interpretation of the data.

The feedback mode of SECM imaging relies on the presence of a redox-active mediator (e.g., $[Ru(NH_3)_6]Cl_3$, $K_3[Fe(CN)_6]$, dissolved O_2) in the electrolyte and the modulation of the amperometric tip current by properties of the sample surface. In the substrate-generator/tip-collector (SG/TC) mode of SECM, the addition of a mediator is intentionally avoided; instead, an appropriately polarized probe tip is used to actively monitor the release or consumption of reducible or oxidizable species at microscopic spots of the sample surface (Figure 7). Metal ion release from sites of localized corrosion, diffusion of electroactive species through narrow pores of semi permeable membranes, O_2 consumption, and release of chemical messengers by single cells are just a few of the many processes that can be assessed in the SG/TC mode of SECM.

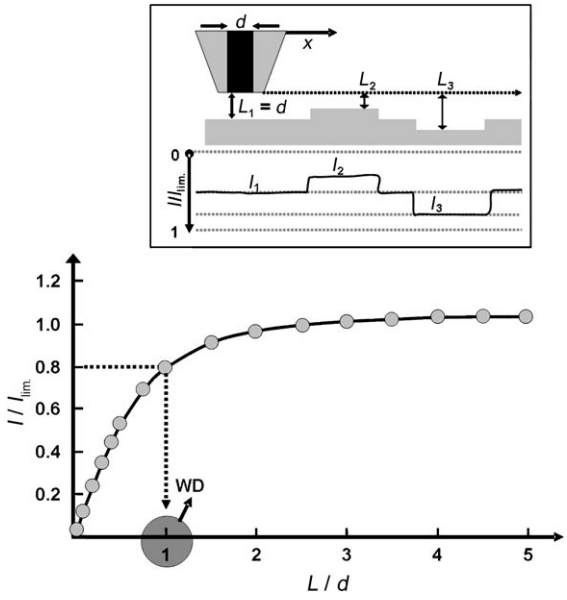

Figure 6. Imaging of the topography of homogeneously insulating samples by means of negative feedback mode SECM. First, an approach curve (normalized tip current vs. normalized tip-to-sample distance) is recorded and used to determine a suitable working distance (WD) for the SECM tip. Usually, distances are chosen at which the amperometric SECM tip current is about 60–80% of its value in bulk solution. The SECM tip is then scanned at the predetermined WD (constant height) in an *x*,*y* plane across the sample surface, and the current is monitored as function of tip position. On homogenously insulating interfaces, variations in the tip current directly reflect variations in the sample topography (top).

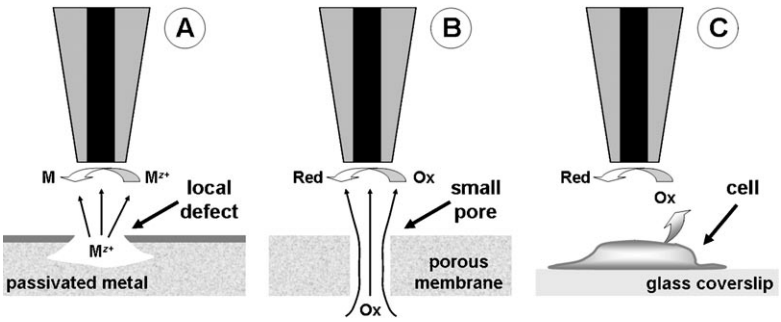

Figure 7. SG/TC mode SECM: An electroactive species may be produced or present at microscopically small active sites on a sample surface. When a suitably polarized SECM tip is scanned over such a "release" site, an increase in the tip current will be observed from the electrochemically induced conversion of the redox species that is delivered locally to the scanned amperometric probe. Examples of processes that can be studied in the SG/TC mode are A) the release of metal ions from locally corroding metals or alloys, B) the diffusion of redox species through the tiny pores of semipermeable membranes and their emergence in the vicinity of the pore opening, and C) the release of readily oxidizable or reducible chemical messenger molecules such as hormones and neurotransmitters from single secretory cells upon stimulation.

5.2. Constant-Height SECM Studies on Single Living Cells

The general setup for single-cell SECM experiments is similar to that shown in Figure 2. The micropositioning device needed to move the SECM tip accurately in the x, y, and z directions is mounted on an inverted microscope to allow optical inspection of the cells and the probe tip. Living cells are typically nonconducting, and for measurements in physiological buffer solutions cells are usually cultured on insulating glass coverslips. Under these conditions, SECM can be applied in negative feedback mode in constant-height scanning experiments to visualize the locations and three-dimensional structures of individual cells. Suitable nontoxic redox mediators or dissolved O_2 may be used to establish the amperometric tip current, which can reflect cellular topography and redox activity.

Figure 8 shows schematically how adherently growing cells can be topographically imaged. After the positions of a target cell and the SECM tip are identified optically, they are aligned near but not on top of each other, and approach curves are recorded with the tip moving slowly towards the surface of the coverslip. If the total diameter of the SECM tip including the insulating sheath is known, approach curves provide a good measure of the absolute tip-to-sample separation distance. The tip can thus be placed just above the glass surface ($I \ll I_\infty$) and then pulled up to a little higher than the predicted diameter of the cell ($I \cong I_\infty$, depending on the size of the UME). Lateral scanning is performed at this preadjusted tip height (fixed z position), and lower amperometric tip currents will be observed above the cell as a result of the increased negative feedback. Plotting the current response as a function of x,y position of the SECM tip offers grayscale or colored SECM images of the examined cells that primarily display topographical information. Further information about cellular redox or secretory activity or the transmembrane fluxes of redox species involved in intracellular processes can usually be obtained from subsequent measurements in SG/TC mode.

SECM studies based on the above strategy have been applied to various cellular processes. Imaging of the topography of single living cells along with O_2 concentrations profiles in their surrounding is one of the earlier examples.[69] Another early study examined the morphology and photosynthetic electron transport of single guard cells.[70] More recent publications include the investigation of the interaction of Ag^+ ions with the respiratory chain of certain bacterial cells and an evaluation of the related antimicrobial effect of μM concentrations of Ag^+ ions,[71] measurements of the cytotoxicity of menadione on hepatoblastoma cells,[72] the detection of the uptake of menadione by yeast cells and its expulsion from them as a glutathione complex,[73] and the characterization of the local respiratory activity of PC12 cells.[74] Liebetrau et al. tested a whole set of redox mediators with respect to their suitability for biological SECM experiments and employed the best ones in constant-height imaging experiments for visualizing the neuronal development of PC12 cells treated with nerve growth factor and detecting changes in cell

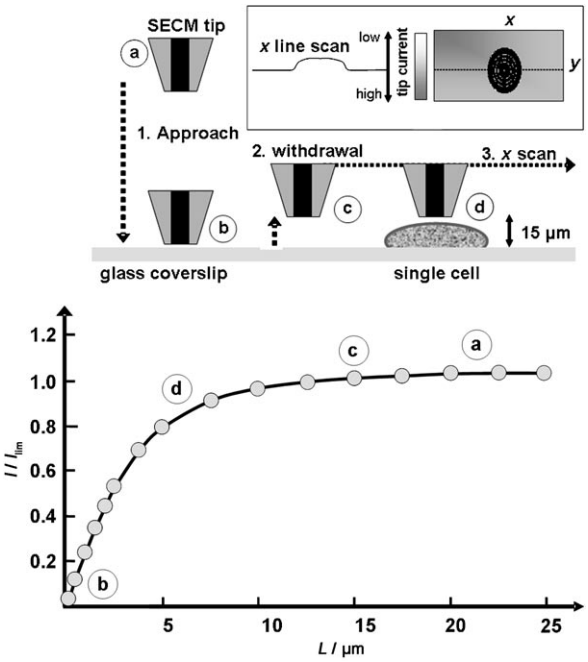

Figure 8. Imaging cell topography using the negative feedback/constant height mode of SECM. An approach curve is recorded in the vicinity of cells with the SECM tip brought carefully from the bulk of solution (position a) towards the surface of the glass coverslip (position b). When the electrode diameter and the ratio between the diameter of the electrode and the insulating glass sheath are known, the approach curve offers an actual measure of the absolute tip-to-surface separation. Imaging the morphology of a cell is then a two-step process: First, the SECM tip is retracted to a distance that is slightly larger than the expected height of the cells to be imaged. This movement may almost reestablish the bulk current (position c). Then, the SECM tip is scanned towards a selected cell, which leads to a current decrease above the living cell as a result of blocking of the diffusion of redox mediator to the electroactive disk (position d). The decrease in the current (ΔI) as seen in plots of I vs. x,y position represents the cell topography.

height induced by exposure to hypotonic or hypertonic buffer solutions in real time.[75]

The work of Mirkin's group on imaging normal and metastatic human breast cells is another example of the potential of single-cell SECM as a modern tool for biomedical analysis and the monitoring of physiologically and pathologically relevant cellular function.[76] Individual breast cells were exposed in physiological saline solution to a chemical mediator (e.g., quinone) that was able to rapidly cross the cell membrane and take part in intracellular redox reactions in the cytoplasm. Changes in extracellular concentrations of the mediator resulting from cytosolic turnovers were monitored on a microsecond timescale by the SECM tip, which was placed close to the cell membrane. Variations in rate constants were observed for cells with different health status and it was shown that they can be used as an indicator for the onset of cell metastasis and identification of single cancerous cells in a field of nontransformed neighbors.

Dual SECM tips with a bare Pt-UME (diameter 10 μm) and a porphyrin-based NO microsensor (diameter 50 μm) located next to each other at the end of pulled and then beveled Θ-shaped glass pipettes have recently been developed for precisely controlling the position of the NO sensor above layers of NO-releasing endothelian cells.[77] With dissolved O_2 as redox mediator, the bare Pt-UME was operated in negative feedback mode, providing a good measure about the distance of the dual-electrode "bifunctional" SECM tip with respect to the surface of the coverslip and the cells. The NO microsensor thus could be carefully guided towards the target cells and placed at an exactly known distance before stimulation and detection of local NO release. With this strategy, it was demonstrated that the acquired NO signals were strongly dependent on the position of the NO sensor relative to the cells (Figure 9). Owing to their relatively large overall tip size, dual-electrode NO-sensitive SECM tips could so far not be applied for lateral scanning on individual cells in the *x*,*y* plane. However, further miniaturization and optimization of the porphyrin-based sensing chemistry[78] may ultimately help to achieve the goal of high-resolution spatial mapping of NO release from specific cells.

The spatial resolution of SECM imaging in the amperometric feedback and the generator/collector mode depends to a large extent on the diameter of the electroactive disk of the SECM tip. Most work is currently performed with SECM tips that have a characteristic diameter and hence suitable working distances between 5 and 10 μm. Because of the relatively wide working range of the feedback mode (relative to the cell height), the methodology for tip positioning shown in Figure 8 works reasonably well with "large" SECM tips, even when the height of the studied cells is not precisely known. However, with decreasing SECM tip diameters, this approach-curve-assisted tip positioning becomes more impractical. Inexact tip placement, however, may lead to a collision into the soft target cells or to the situation whereby negative feedback is not achieved above the cell and thus SECM imaging is obstructed. In the next section, the recent efforts to circumvent the problem are discussed and strategies for current-independent tip positioning are described.

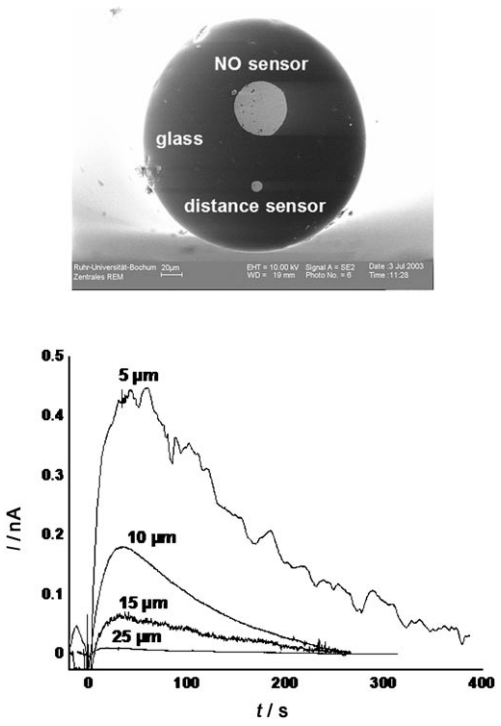

Figure 9. Employment of dual-disk, bifunctional SECM probes for the reproducible and accurate positioning of NO-specific sensors at known distances from NO-releasing cells. Top: One of the two electrodes, a bare Pt disk electrode (diameter 10 μm), is operated as a conventional amperometric SECM tip and thus can be used with feedback-mode *z*-approach curves as a guide for the slightly larger second electrode, a metal-porphyrin- or metal-phthalocyanine-modified Pt disk (diameter 50 μm). Bottom: A set of stimulated NO-release measurements made at various distances between the disk surface of the NO microsensor and the endothelial cells. The magnitude of the acquired NO signals is strongly dependent on the position of the NO sensor relative to the release sites. Reproduced with permission from reference [77a].

5.3. Constant-Distance Mode SECM on Single Living Cells

SECM has the potential for imaging the topography of single cells along with their chemical activity, and, if the current trend of technical improvements continues, should in the future become the tool of choice for elucidating the relations between local structural and chemical properties as well as functional performances such as cell growth and degeneration. PC12 cells, for example, differentiate and start to form neurites, varicosities, and complex connections to neighboring cells when they are treated in the culture medium with a stimulating nerve growth factor. SECM in that case could monitor the process of cell development over time and track the morphological changes at different stages of differentiation along with the local chemical profiles of species in the surrounding of gradually appearing cellular substructures. However, an essential prerequisite for optimal spatial resolution is the use of the smallest possible UMEs as the scanning probes. Ideally, the miniaturized SECM tips should be guided smoothly in close and constant distance over the generally irregular surface of the cells (Figure 10). This approach was

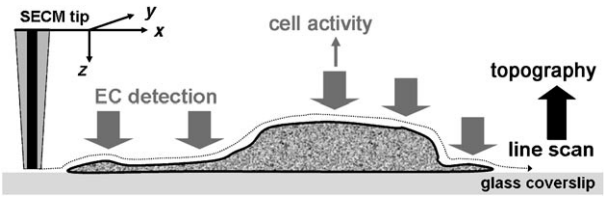

Figure 10. The study of living cells in the constant-distance mode SECM. In line scans, the SECM tip is guided at constant distance over an individual cell. The readings of the *z*-positioning device, which responds to local variations in the landscape of the scanned surface by either retracting or extending the tip, provide an accurate measure of the sample topography (dotted line). The topographic information contained in constant-distance line scans may be used to position the SECM tip at distinct locations above (substructures of) a cell where electrochemical detection of cellular processes can then be performed.

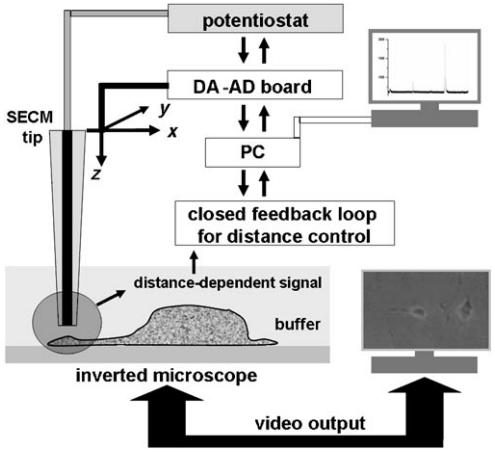

Figure 11. Schematic diagram of a biological scanning electrochemical microscope for high-resolution constant-distance mode SECM topographical and chemical imaging of single living cells. The instrument consists of the SECM tip, a micropositioning device for precise SECM tip movement, an inverted optical microscope with optional video output for visualizing the probe tip and cells, a distance-control unit with a computer-controlled feedback loop, a low-noise potentiostat, and a PC connected to a DA–AD board. A micropipette-based injection system, needed for local application of stimulatory agents, is not shown.

proposed not only for nondestructive tip positioning at soft and microscopically small objects, but also for the acquisition of topographic information through the settings of the *z*-micropositioning device. In the proposed constant-distance mode of SECM, the recorded *z* position during the *x*,*y* line scans reflects the topography of the sample. Electrochemical data may be either recorded continuously during scanning or taken with a stationary tip that was precisely placed at an interesting location at the cell surface through the repetition of an acquired line scan.

Constant-distance mode SECM imaging requires computer-controlled feedback circuitry that continuously compares a distance-dependent signal from the SECM tip with a user-defined value and repositions the tip when deviations are detected. Several schemes have been proposed for obtaining the distance-dependent input signal to be applied to the feedback loop of the distance-control unit of an SECM instrument. One is the use of a shear-force-based feedback mechanism with optical,[79] piezoelectric,[80] or tuning-fork-based[81] detection of the short-range hydrodynamic shear forces that suddenly occur between an in resonance vibrating SECM tip and the sample surface at distances below 100–300 nm. Other approaches are based on the maintenance of a constant amperometric SECM tip current during scanning[81d,82] or employ the tip impedance[82a,83] as a feedback signal.

A technically very different approach for simultaneous electrochemical and topographical imaging with constant-distance scanning is the implementation of SECM in atomic force microscopes by using specially designed AFM cantilevers with partially insulated metal tips as microelectrodes.[84] The bifunctional AFM tips are designed to act as both the force sensor for topographical imaging and as the UME for microelectrochemical measurements.

The various SECM distance-control units have their advantages and disadvantages and, with the exception of the piezoelectric detection of shear forces and combined AFM/SECM, have been demonstrated to be feasible for topographic imaging of individual living cells. An advantage of using shear forces or the tip impedance instead of an amperometric tip current as the feedback signal is that the presence of possibly toxic exogenous redox mediators in the physiological buffer solution can be avoided. Figure 11 displays a schematic representation of a typical biological constant-distance SECM ("Bio-SECM"). The setups proposed so far are basically similar in their design and are composed of a distance-control unit, the micropositioning devices, the tip holder, and an electrochemical cell, all of which are arranged on the stage of a high-quality inverted microscope to satisfy the requirements of physiological-electrochemical experiments.

In the first published applications of constant-distance Bio-SECM, the instrument was used for combined topography and secretion measurements on individual PC12 and chromaffin cells. Conventionally sized CF-UMEs with a tip diameter of about 5 μm[82a,85] and electrochemically etched and electropainted CF-UMEs with significantly reduced tip diameters of 1–2 μm[85] were operated in constant-distance mode to reveal first the details of the topography of an individual secretory cell and then use this information for placing the SECM tip directly above the center of the cell. Figure 12 shows a typical recording. The precise positioning of the SECM tip at a distance of 100–300 nm from the cell membrane subsequently allowed the local detection of vesicular chemical release, initiated by the addition of a stimulant and known from conventional carbon-fiber amperometry.

More recently, conical electrodes were made from optical fiber and glass capillaries by coating the outside of pulled glass tips with metal and then insulating the conducting surface tips by means of vapor deposition with an insulating polymer. These electrodes were operated in constant-distance mode SECM for simultaneous topographical, optical, and electrochemical imaging of stained PC12 cells and allowed visualization of the respiratory activity in the electrochemical

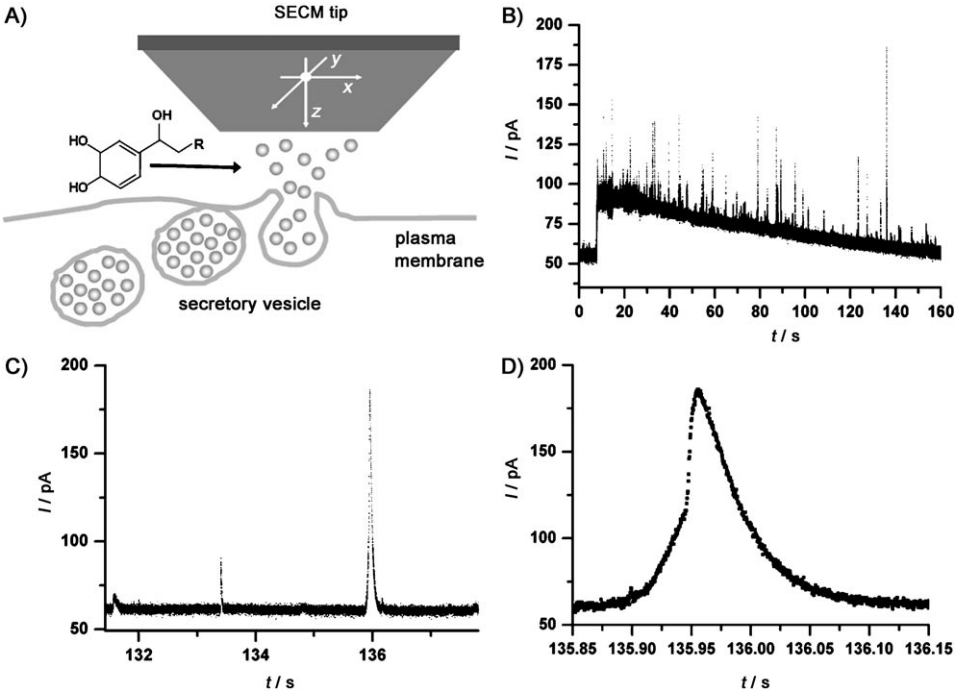

Figure 12. A) Application of constant-distance mode biological scanning electrochemical microscopy (Bio-SECM) for the local amperometric detection of single-vesicle adrenaline release from an individual bovine chromaffin cell. With the topography known from shear-force-based constant-distance mode line scans, the SECM tip, in this case a carbon-fiber disk electrode (diameter 5 μm, polarized to +800 mV vs. Ag/AgCl), was placed at a distance less than 1 μm directly above the center of a single bovine chromaffin cell. B) When the selected cell was stimulated with 100 mM KCl solution, exocytosis was initiated and detected with excellent sensitivity by the appearance of a large number of pA current spikes in the amperometric SECM tip current, each representing chemical release from an individual secretory granule. C,D) Expanded sections of (B) with higher temporal resolution. Reproduced with permission from reference [86].

images.[81a] Also, very sensitive Ni–phthalocyanine-modified CF-UMEs were constructed for the local detection of NO and implemented in constant-distance SECM.[87] Again, constant-distance positioning of the tip was employed to position the NO microsensor directly above an adherently growing human umbilical vein endothelian cell (HUVEC cell). NO release was then stimulated by the application of bradykinin, leading to a current increase at the NO microsensor, which was kept at a constant potential of 750 mV versus Ag/AgCl (Figure 13).

The development of the constant-distance mode of SECM and the outcome of the above-mentioned experiments on catecholamine- and NO-secreting cells should be seen as the early steps towards the ambitious goal of spatial and chemical SECM mapping of (networks of) living cells. The miniaturization of the electrochemical scanning probes and optimization of the performance of the distance control must be the next steps for Bio-SECM to allow an assessment of the structure–function relationship in cellular microenvironments with superior spatial resolution.

6. Conclusion and Future Aspects

Individual cells are the microscopically small operational subunits of living beings. Throughout the mammalian body, for example, these objects form a network of gigantic architectural and functional complexity. Many cell types are heavily involved in harmoniously orchestrating the molecular machinery of life, such as the large number of different neurons in the central and peripheral nervous system, including the brain and the many secretory cells of the endocrine system. As highlighted in this article, tiny but powerful accurately movable voltammetric UMEs have been developed into highly sophisticated analytical tools for the analysis of the multifaceted chemistry in the close surrounding of single cells. This progress in single-cell voltammetry in little more than two decades became possible thanks to the joint efforts of researchers in the areas of electrochemistry, medicine, and biology.

The evaluation of quantal neurotransmitter release from isolated neuronal and endocrine cells with a temporal and spatial resolution sufficient for visualizing the secretory activity of single intracellular storage vesicles of nanometer dimension, as well as the success of biological scanning electrochemical microscopy for the simultaneous imaging of topography and chemical (redox) activity of adherent cells are prominent milestones in cellular microelectroanalysis. Nonetheless, even when all the achievements up to the present time are taken into account, single-cell microelectrochemistry has not yet reached the zenith of its potential for exploring mechanisms behind cell development and degeneration or for studying processes such as cell-to-cell communication and synaptogenesis. Until now, most of the works on cultured cells and cells in tissue slices has involved micrometer-sized voltammetric sensors. The next goal will be the routine fabrication of highly sensitive nanometer-sized electrochemical probe tips and their high precision position not only around single cells but also along more complicated networks of cells. Other challenges include the further optimization of the soft- and hardware that controls and synchronizes tip movement and the electrochemical data acquisition, as well as the development of selective nanoelectrode tips for relevant target analytes other than those that can be easily detected through their direct oxidation or reduction. It will be exciting to see which results in another two decades, after the above-mentioned technical and methodical improvements are (to some extent) in place, might then be reviewed as "single-cell nanoelectrochemistry" and with which techniques the chem-

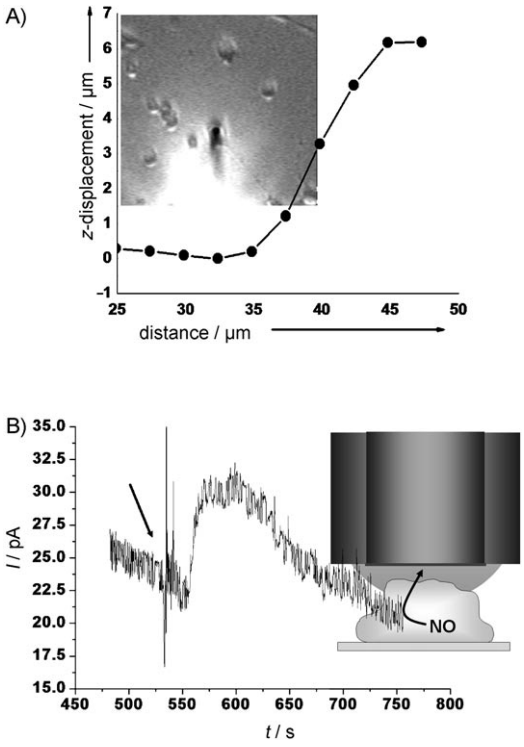

Figure 13. A) Shear-force-based constant-distance line scan used for positioning the NO microsensor exactly above a single human umbilical vein endothelian (HUVEC) cell. The inset shows the shadow of the microsensor above the selected single cell in a simultaneously acquired video microscope image. B) Amperometric detection of NO released from a single HUVEC cell upon stimulation with bradykinin. Reproduced with permission from reference [87].

ical communication of and between individual cells in response to physiological, pathological, or pharmacological stimulation may be routinely monitored in life science laboratories.

Received: November 30, 2006
Published online: October 19, 2007

[1] K. Stulik, C. Amatore, K. Holub, V. Marecek, W. Kutner, *Pure Appl. Chem.* **2000**, *72*, 1483 – 1492.
[2] *Microelectrodes: Theory and Application*, *NATO ASI Series E197* (Eds.: M. I. Montenegro, M. A. Queiros, J. L. Daschbach), Kluver, Dordrecht, **1991**.
[3] a) C. Amatore, E. Maisonhaute, *Anal. Chem.* **2005**, *77*, 303A – 311A; b) C. G. Zoski, *Electroanalysis* **2002**, *14*, 1041 – 1051; c) M. Ciszkowska, Z. Stojek, *Anal. Chem.* **2000**, *72*, 754A – 760A; d) R. J. Foster, *Chem. Soc. Rev.* **1994**, *23*, 289 – 297; e) J. Heinze, *Angew. Chem.* **1993**, *105*, 1327 – 1349; *Angew. Chem. Int. Ed. Engl.* **1993**, *32*, 1268 – 1288; f) K. Aoki, *Electroanalysis* **1993**, *5*, 627 – 639; g) H.-P. Nirmaier, G. Henze, *Electroanalysis* **1997**, *9*, 619 – 624; h) R. M. Wightman, *Anal. Chem.* **1981**, *53*, A1125 – A1134.
[4] a) R. N. Adams, *Prog. Neurobiol.* **1990**, *35*, 297 – 311; b) J. O. Schenk, E. Miller, M. E. Rice, R. N. Adams, *Brain Res.* **1983**, *277*, 1 – 8; c) H.-Y. Cheng, J. Schenk, R. Huff, R. N. Adams, *J. Electroanal. Chem. Interfacial Electrochem.* **1979**, *100*, 23 – 31; d) R. L. McCreery, R. Dreiling, R. N. Adams, *Brain Res.* **1974**, *73*, 15 – 21; e) P. T. Kissinger, J. B. Hart, R. N. Adams, *Brain Res.* **1973**, *55*, 209 – 213.
[5] a) M. Fillenz, *Neurosci. Biobehav. Rev.* **2005**, *29*, 949 – 962; b) D. L. Robinson, B. J. Venton, M. L. A. V. Heien, R. M. Wightman, *Clin. Chem.* **2003**, *49*, 1763 – 1773; c) P. E. M. Phillips, R. M. Wightman, *Trends Anal. Chem.* **2003**, *22*, 509 – 514; d) K. P. Troyer, M. L. A. V. Heien, B. J. Venton, R. M. Wightman, *Curr. Opin. Chem. Biol.* **2002**, *6*, 696 – 703; e) J. A. Stamford, J. B. Justice, *Anal. Chem.* **1996**, *68*, 359A – 363A; f) R. D. O'Neill, *Analyst* **1994**, *119*, 767 – 779; g) J. A. Stamford, *J. Neurosci. Methods* **1986**, *17*, 1 – 29; h) J. A. Stamford, *Brain Res.* **1985**, *357*, 119 – 135.
[6] a) F. Crespi, D. Dalessandro, V. Annovazzi-Lodi, C. Heidbreder, M. Norgia, *J. Neurosci. Methods* **2004**, *140*, 153 – 161; b) P. A. Garris, R. Ensmann, J. Poehlman, A. Alexander, P. E. Langley, S. G. Sandberg, P. G. Greco, R. M. Wightman, G. V. Rebec, *J. Neurosci. Methods* **2004**, *140*, 103 – 115; c) M. G. De Simoni, A. De Luigi, L. Imeri, S. Algeri, *J. Neurosci. Methods* **1990**, *33*, 233 – 240; d) V. Annovazzi-Lodi, S. Donati, *IEEE Trans. Biomed. Eng.* **1988**, *35*, 595 – 606.
[7] B. J. Venton, R. M. Wightman, *Anal. Chem.* **2003**, 414A – 421A.
[8] a) G. D. Stuber, R. M. Wightman, R. M. Carelli, *Neuron* **2005**, *46*, 661 – 669; b) M. F. Roitman, G. D. Stuber, P. E. M. Phillips, R. M. Wightman, R. M. Carelli, *J. Neurosci.* **2004**, *24*, 1265 – 1271; c) P. G. Greco, P. A. Garris, *Eur. J. Pharmacol.* **2003**, *479*, 117 – 125; d) P. E. M. Phillips, G. D. Stuber, M. L. Helen, R. M. Wightman, R. M. Carelli, *Nature* **2003**, *422*, 614 – 618; e) R. M. Wightman, D. L. Robinson, *J. Neurochem.* **2002**, *82*, 721 – 735; f) D. L. Robinson, P. E. M. Phillips, E. A. Budygin, B. J. Trafton, P. A. Garris, R. M. Wightman, *Neuroreport* **2001**, *12*, 2549 – 2552; g) M. R. Kilpatrick, M. B. Rooney, D. J. Michael, R. M. Wightman, *Neuroscience* **2000**, *96*, 697 – 706; h) G. V. Rebec, J. R. Christensen, C. Guerra, M. T. Bardo, *Brain Res.* **1997**, *776*, 61 – 67.
[9] a) D. J. Stephens, V. J. Allan, *Science* **2003**, *300*, 82 – 86; b) W. R. Zipfel, R. M. Williams, W. W. Webb, *Nat. Biotechnol.* **2003**, *21*, 1369 – 1377; c) E. S. Yeung, *Anal. Chem.* **1999**, *71*, A522 – A529; d) M. Dailey, G. Marrs, J. Satz, M. Waite, *Biol. Bull.* **1999**, *197*, 115 – 122.
[10] a) *Single-Channel Recording*, *2nd ed.* (Eds.: B. Sakmann, E. Neher), Kluwer, Dordrecht, **1995**; b) *Microelectrode techniques*, *The Plymouth workshop handbook*, *2nd ed.* (Ed.: D. C. Ogden), Company of Biologists, Cambridge, **1994**.
[11] R. Feeney, S. P. Kounaves, *Electroanalysis* **2000**, *12*, 677 – 684.
[12] I. Hafez, K. Kisler, K. Berberian, G. Demick, V. Valero, M. G. Yong, H. G. Craighead, M. Lindau, *Proc. Natl. Acad. Sci. USA* **2005**, *102*, 13879 – 13884.
[13] a) H.-F. Cui, J.-S. Shan, Y. Chen, S.-C. Chong, X. Liu, T.-M. Lim, F.-S. Sheu, *Sens. Actuators B* **2006**, *115*, 634 – 641; b) T. S. Strong, H. C. Cantor, R. B. Brown, *Sens. Actuators A* **2001**, *91*, 357 – 362.
[14] S. Isik, L. Berdondini, J. Oni, A. Bloechl, M. Koudelka-Hep, W. Schuhmann, *Biosens. Bioelectron.* **2005**, *20*, 1566 – 1572.
[15] a) A. J. Bard, F. R. F. Fan, J. Kwak, O. Lev, *Anal. Chem.* **1989**, *61*, 132 – 138; b) R. C. Engstroem, M. Weber, D. J. Wunder, R. Burgess, S. Winquist, *Anal. Chem.* **1986**, *58*, 844 – 848.
[16] a) M. A. Edwards, S. Martin, A. L. Whitworth, J. V. Macpherson, P. R. Unwin, *Physiol. Meas.* **2006**, *27*, R63 – R108; b) A. J. Bard, X. Li, W. Zhan, *Biosens. Bioelectron.* **2006**, *22*, 461 – 472; c) S. Amemiya, J. D. Guo, H. Xiong, D. A. Gross, *Anal. Bioanal. Chem.* **2006**, *386*, 458 – 471; d) M. Navratil, G. A. Mabbott, E. A. Arriaga, *Anal. Chem.* **2006**, *78*, 4005 – 4019; e) B. F. Brehm-Stecher, E. A. Johnson, *Microbiol. Mol. Biol. Rev.* **2004**, *68*, 538 – 559; f) T. Yasukawa, T. Kaya, T. Matsue, *Electroanalysis* **2000**, *12*, 653 – 659.
[17] R. S. Kelly, R. M. Wightman, *Anal. Chim. Acta* **1986**, *187*, 79 – 87.
[18] R. H. Chow, L. Von Rueden, E. Neher, *Nature* **1992**, *356*, 60 – 63.

[19] A. Schulte, R. H. Chow, *Anal. Chem.* **1996**, *68*, 3054 – 3058.
[20] a) S. Chen, A. Kucernak, *Electrochem. Commun.* **2002**, *4*, 80 – 85; b) M. S. Mousa, *Appl. Surf. Sci.* **1996**, *94/95*, 129 – 135; c) A. Schulte, PhD thesis, Westfälische Wilhelms-Universität Münster (Germany), **1994**; d) J. O. Besenhard, A. Schulte, K. Schur, P. D. Jannakoudakis in *Microelectrodes: Theory and Application*, *NATO ASI Series E197* (Eds.: M. I. Montenegro, M. A. Queiros, J. L. Daschbach), Kluver, Dordrecht, **1991**, pp. 189 – 204.
[21] J. Millar, C. W. A. Pelling, *J. Neurosci. Methods* **2001**, *110*, 1 – 8.
[22] a) W.-Z. Wu, W.-H. Huang, W. Wang, Z.-L. Wang, J.-K. Cheng, T. Xu, R.-Y. Zhang, Y. Chen, J. Liu, *J. Am. Chem. Soc.* **2005**, *127*, 8014 – 8915; b) W.-H. Huang, D.-W. Pang, H. Tong, Z.-L. Wang, J.-K. Chen, *Anal. Chem.* **2001**, *73*, 1048 – 1052; c) T. G. Strein, A. G. Ewing, *Anal. Chem.* **1992**, *64*, 1368 – 1373.
[23] X. Zhang, W. Zhang, X. Zhou, B. Ogorevc, *Anal. Chem.* **1996**, *68*, 3338 – 3343.
[24] A. Schulte, R. H. Chow, *Anal. Chem.* **1998**, *70*, 985 – 990.
[25] D. K. Y. Wong, L. Y. F. Xu, *Anal. Chem.* **1995**, *67*, 4086 – 4090.
[26] a) D. D. Yao, A. G. Vlessidis, N. P. Evmiridis, *Microchim. Acta* **2004**, *147*, 1 – 20; b) Z. H. Taha, *Talanta* **2003**, *61*, 3 – 10; c) F. Bedioui, N. Villeneuve, *Electroanalysis* **2003**, *15*, 5 – 18; d) L. Huang, R. T. Kennedy, *Trends Anal. Chem.* **1995**, *14*, 158 – 164.
[27] a) C. Wang, X. Hu, *Talanta* **2006**, *68*, 1322 – 1328; b) C. J. Slevin, N. J. Gray, J. V. Macpherson, M. A. Webb, P. R. Unwin, *Electrochem. Commun.* **1999**, *1*, 282,-288; c) B. Ballesteros Katemann, W. Schuhmann, *Electroanalysis* **2002**, *14*, 22 – 28; d) B. D. Pendley, H. D. Abruna, *Anal. Chem.* **1990**, *62*, 782 – 784.
[28] S. C. Land, D. M. Porterfield, R. H. Sanger, P. J. S. Smith, *J. Exp. Biol.* **1999**, *202*, 211 – 218.
[29] W. J. Whalen, J. Riley, P. Nair, *J. Appl. Physiol.* **1967**, *23*, 798 – 801.
[30] a) Y. Y. Lau, J. B. Chien, D. K. Y. Wong, A. G. Ewing, *Electroanalysis* **1991**, *3*, 87 – 95; b) Y. T. Kim, D. M. Scarnulis, A. G. Ewing, *Anal. Chem.* **1986**, *58*, 1782 – 1786.
[31] J. B. Chien, R. A. Wallingford, A. G. Ewing, *J. Neurochem.* **1990**, *54*, 633 – 638.
[32] Y. Y. Lau, T. Abe, A. G. Ewing, *Anal. Chem.* **1992**, *64*, 1702 – 1705.
[33] a) T. Abe, Y. Y. Lau, A. G. Ewing, *Anal. Chem.* **1992**, *64*, 2160 – 2163; b) T. Abe, Y. Y. Lau, A. G. Ewing, *J. Am. Chem. Soc.* **1991**, *113*, 7421 – 7423.
[34] A. Meulemans, B. Poulain, G. Baux, L. Tauc, *Brain Res.* **1987**, *414*, 158 – 162.
[35] A. Meulemans, B. Poulain, G. Baux, L. Tauc, D. Henzel, *Anal. Chem.* **1986**, *58*, 2088 – 2091.
[36] T. Malinski, Z. Taha, *Nature* **1992**, *358*, 676 – 678.
[37] T. Malinski, S. Grunfeld, Z. Taha, P. Tomboulian, *Environ. Health Perspect.* **1994**, *102*, 147 – 151.
[38] J. B. Chien, R. A. Saraceno, A. G. Ewing, *Redox Chem. Interfacial Behav. Biol. Mol. [Proc. Int. Symp. Redox Mech. Interfacial Prop. Mol. Biol. Importance] 3rd* (1988), Meeting Date 1987, Plenum, New York, **1988**, 417 – 424.
[39] a) E. Neher, *Pfluegers Arch.* **2006**, *453*, 261 – 268; b) M. B. Jackson, E. R. Chapman, *Annu. Rev. Biophys. Biomol. Struct.* **2006**, *35*, 135 – 160; c) R. Schneggenburger, E. Neher, *Curr. Opin. Neurobiol.* **2005**, *15*, 266 – 274; d) J. W. Barclay, A. Morgan, R. D. Burgoyne, *Cell Calcium* **2005**, *38*, 343 – 353; e) J. B. Sorensen, *Trends Neurosci.* **2005**, *28*, 453 – 455; f) T. C. Suedhof, *Annu. Rev. Neurosci.* **2004**, *27*, 509 – 547; g) T. F. J. Martin, *Biochim. Biophys. Acta* **2003**, *1641*, 157 – 165; h) W. C. Tucker, E. R. Chapman, *Biochem. J.* **2002**, *366*, 1 – 13; i) R. Jahn, T. C. Suedhof, *Annu. Rev. Neurosci.* **1994**, *17*, 219 – 246; j) R. D. Burgoyne, A. Morgan, *Physiol. Rev.* **2003**, *83*, 581 – 632; k) W. J. Betz, J. K. Angleson, *Annu. Rev. Physiol.* **1998**, *60*, 347 – 363; l) P.-M. Lledo, *Eur. J. Endocrinol.* **1997**, *137*, 1 – 9; m) R. S. Zucker, *Neuron* **1996**, *17*, 1049 – 1055; n) T. C. Suedhof, *Nature* **1995**, *375*, 645 – 653.
[40] a) J. F. Presley, *Biochim. Biophys. Acta Mol. Cell Res.* **2005**, *1744*, 259 – 272; b) H. B. Pollard, D. K. Apps, *Ann. N. Y. Acad. Sci.* **2002**, *971*, 617 – 619; c) M. Oheim, D. Loerke, R. H. Chow, W. Stuehmer, *Philos. Trans. R. Soc. London Ser. B* **1999**, *354*, 307 – 318; d) J. A. Steyer, A. Horstmann, W. Almers, *Nature* **1997**, *388*, 474 – 478; e) M. Oheim, D. Loerke, W. Stuehmer, R. H. Chow, *Eur. Biophys. J.* **1998**, *27*, 83 – 98.
[41] a) R. Heidelberger, *Rev. Physiol. Biochem. Pharmacol.* **2001**, *143*, 1 – 80; b) "Techniques for membrane capacitance measurements": K. D. Gillis in *Single-Channel Recording*, *2nd ed.* (Eds. B. Sakmann, E. Neher), Plenum, New York, **1995**, pp. 155 – 188; c) G. Matthews, *Curr. Opin. Neurobiol.* **1996**, *6*, 358 – 364; d) M. Lindau, E. Neher, *Pflügers Arch.* **1988**, *411*, 137 – 146.
[42] a) E. V. Mosharov, D. Sulzer, *Nat. Methods* **2005**, *2*, 651 – 658; b) R. H. S. Westerink, *Neurotoxicology* **2004**, *25*, 461 – 470; c) D. Bruns, *Methods* **2004**, *33*, 312 – 321; d) D. M. Cannon, Jr., N. Winograd, A. G. Ewing, *Annu. Rev. Biophys. Biomol. Struct.* **2000**, *29*, 239 – 263; e) J. P. Henry, F. Darchen, S. Cribier, *Biochimie* **1998**, *80*, 371 – 377; f) E. R. Travis, R. M. Wightman, *Annu. Rev. Biophys. Biomol. Struct.* **1998**, *27*, 77 – 103; g) J. K. Angleson, W. J. Betz, *Trends Neurosci.* **1997**, *20*, 281 – 287; h) G. Y. Chen, A. G. Ewing, *Crit. Rev. Neurobiol.* **1997**, *11*, 59 – 90; i) R. M. Wightman, J. M. Finnegan, K. Pihel, *Trends Anal. Chem.* **1995**, *14*, 154 – 158; j) E. Neher, R. H. Chow, *Bioelectrochem. Bioenerg.* **1995**, *2*, 251 – 253; k) A. G. Ewing, T. G. Strein, Y. Y. Lau, *Acc. Chem. Res.* **1992**, *25*, 440 – 447.
[43] a) D. J. Leszczyszyn, J. A. Jankowski, O. H. Viveros, E. J. Diliberto, Jr., J. A. Near, R. M. Wightman, *J. Biol. Chem.* **1990**, *265*, 14736 – 14737; b) M. R. Duchen, J. Millar, T. J. Biscoe, *J. Physiol.* **1990**, *426*, 5P.
[44] R. H. Chow, L. von Rueden, E. Neher, *Nature* **1992**, *356*, 60 – 63.
[45] a) J. F. Gómez, M. A. Brioso, J. D. Machado, J. L. Sanchez, R. Borges, *Ann. N. Y. Acad. Sci.* **2002**, *971*, 647 – 654; b) F. Segura, M. A. Brioso, J. F. Gómez, J. D. Machado, R. Borges, *J. Neurosci. Methods* **2000**, *103*, 151 – 156; c) A. Elhamdani, Z. Zhou, C. R. Artalejo, *J. Neurosci.* **1998**, *18*, 6230 – 6240; d) A. Elhamdani, T. F. J. Martin, J. A. Kowalchyk, C. R. Artalejo, *J. Neurosci.* **1999**, *19*, 7375 – 7383.
[46] a) M. L. A. V. Heien, M. A. Johnson, R. M. Wightman, *Anal. Chem.* **2004**, *76*, 5697 – 5704; b) D. J. Michael, J. D. Joseph, M. R. Kilpatrick, E. R. Travis, R. M. Wightman, *Anal. Chem.* **1999**, *71*, 3941 – 3947; c) B. P. Jackson, S. M. Dietz, R. M. Wightman, *Anal. Chem.* **1995**, *67*, 1115 – 1120; d) J. A. Stamford, *J. Neurosci. Methods* **1990**, *34*, 67 – 72.
[47] a) D. S. Koh, *Methods Mol. Biol.* **2006**, *337*, 139 – 153; b) K. T. Kim, D. S. Koh, B. Hille, *J. Neurosci.* **2000**, *20*, 1 – 5.
[48] a) G. Nagy, J. H. Kim, Z. P. Pang, U. Matti, J. Rettig, T. C. Suedhof, J. B. Sorensen, *J. Neurosci.* **2006**, *26*, 632 – 643; b) C. L. Haynes, L. A. Buhler, R. M. Wightman, *Biophys. Chem.* **2006**, *123*, 20 – 24; c) J. R. Constable, M. E. Graham, A. Morgan, R. D. Burgoyne, *J. Biol. Chem.* **2005**, *280*, 31615 – 31623; d) C. Amatore, S. Arbault, I. Bonifas, Y. Bouret, M Erard, A. G. Ewing, L. A. Sombers, *Biophys. J.* **2005**, *88*, 4411 – 4420; e) D. Speidel, C. E. Bruederle, C. Enk, T. Voets, F. Varoqueaux, K. Reim, U. Becherer, F. Fornai, S. Ruggieri, Y. Hollighaus, E. Weihe, D. Bruns, N. Brose, J. Rettig, *Neuron* **2005**, *46*, 75 – 88; f) X.-K. Chen, L.-C. Wang, Y. Zhou, Q. Cai, M. Prakriya, K.-L. Duan, Z.-H. Sheng, C. Lingle, Z. Zhou, *Nat. Neurosci.* **2005**, *8*, 1160 – 1168; g) G. Nagy, K. Reim, U. Matti, N. Brose, T. Binz, J. Rettig, E. Neher, J. B. Sorensen, *Neuron* **2004**, *41*, 351 – 365; h) C. Amatore, S. Arbault, I. Bonifas, Y. Bouret, M Erard, M. Guille, *ChemPhysChem* **2003**, *4*, 147 – 154; i) J. B. Sorensen, R. Fernandez-Chacon, T. C. Suedhof, E. Neher, *J. Gen. Physiol.* **2003**, *122*, 265 – 276; j) C. Amatore, Y. Bouret, E. R. Travis, R. M. Wightman, *Biochimie* **2000**, *82*, 481 – 496; k) M. E. Graham, P. Washbourne, M. C. Wilson, R. D. Burgoyne, *Ann.*

N. Y. Acad. Sci. **2002**, *971*, 210 – 221; l) T. L. Colliver, E. J. Hess, A. G. Ewing, *J. Neurosci. Methods* **2001**, *105*, 95 – 103; m) T. Voets, T. Moser, P.-E. Lund, R. H. Chow, M. Geppert, T. C. Suedhof, E. Neher, *Proc. Natl. Acad. Sci. USA* **2001**, *98*, 11680 – 11685; n) M. Haller, C. Heinemann, R. H. Chow, R. Heidelberger, E. Neher, *Biophys. J.* **1998**, *74*, 2100 – 2113; o) A. F. Oberhauser, I. M. Robinson, J. M. Fernandez, *Biophys. J.* **1996**, *71*, 1131 – 1139; p) R. H. Chow, J. Klingauf, E. Neher, *Proc. Natl. Acad. Sci. USA* **1994**, *91*, 12765 – 12769.

[49] a) J. M. Moore, J. B. Papke, A. L. Cahill, A. B. Harkins, *Am. J. Physiol.* **2006**, *291*, C270 – C281; b) L. A. Sombers, H. J. Hanchar, T. L. Colliver, N. Wittenberg, A. Cans, S. Arbault, C. Amatore, A. G. Ewing, *J. Neurosci.* **2004**, *24*, 303 – 309; c) J. Bai, C.-T. Wang, D. A. Richards, M. B. Jackson, E. R. Chapman, *Neuron* **2004**, *41*, 929 – 941; d) J. M. Finnegan, K. Pihel, P. S. Cahill, L. Huang, S. E. Zerby, A. G. Ewing, R. T. Kennedy, R. M. Wightman, *J. Neurochem.* **1996**, *66*, 1914 – 1923; e) T. K. Chen, G. Luo, A. G. Ewing, *Anal. Chem.* **1994**, *66*, 3031 – 3035.

[50] a) E. H. Jaffe, P. Bulanos, C. Caputo, *Cell Calcium* **2001**, *29*, 199 – 209; b) K. Pihel, S. Hsieh, J. W. Jorgensen, R. M. Wightman, *Biochemistry* **1998**, *37*, 1046 – 1052; c) A. F. Oberhauser, I. M. Robinson, J. M. Fernandez, *Biophys. J.* **1996**, *71*, 1131 – 1139; d) P. E. Tatham, M. R. Duchen, J. Millar, *Pflugers Arch.* **1991**, *419*, 409 – 414.

[51] a) D. J. Michael, R. A. Ritzel, L. Haataja, R. H. Chow, *Diabetes* **2006**, *55*, 600 – 607; b) K. Bokvist, M. Holmqvist, J. Gromada, P. Rorsman, *Pflugers Arch.* **2000**, *439*, 634 – 645; c) C. A. Aspinwall, L. Huang, J. R. Lakey, R. T. Kennedy, *Anal. Chem.* **1999**, *71*, 5551 – 5556; d) L. Huang, H. Shen, M. A. Atkinson, R. T. Kennedy, *Proc. Natl. Acad. Sci. USA* **1995**, *92*, 9608 – 9612; e) R. T. Kennedy, L. Huang, M. A. Atkinson, P. Dush, *Anal. Chem.* **1993**, *65*, 1882 – 1887.

[52] V. S. Tran, A. M. Marion-Audibert, E. Karatekin, S. Huet, S. Cribier, K. Guillaumie, C. Chapuis, C. Desnos, F. Darchen, J. P. Henry, *Ann. N. Y. Acad. Sci.* **2004**, *1014*, 179 – 188.

[53] S. Iwaki, M. Ogasawara, R. Kurita, O. Niwa, K. Tanizawa, Y. Ohashi, K. Maeyama, *Anal. Biochem.* **2002**, *304*, 236 – 243.

[54] X. Chen, L. Wang, Y. Zhou, L.-H. Zheng, Z. Zhou, *J. Neurosci.* **2005**, *25*, 9236 – 9243.

[55] a) R. G. Staal, E. V. Mosharov, D. Sulzer, *Nat. Neurosci.* **2004**, *7*, 341 – 346; b) E. N. Pothos, V. Davila, D. Sulzer, *J. Neurosci.* **1998**, *18*, 4106 – 4118; c) B. B. Anderson, A. G. Ewing, *J. Pharmacol. Biomed. Anal.* **1999**, *19*, 15 – 32; d) D.-S. Koh, B. Hille, *Proc. Natl. Acad. Sci. USA* **1997**, *94*, 1506 – 1511; e) Z. Zhou, S. Misler, *Proc. Natl. Acad. Sci. USA* **1995**, *92*, 6938 – 6942; f) D. Bruns, R. Jahn, *Nature* **1995**, *377*, 62 – 65.

[56] G. Arroyo, J. Fuentealba, N. Sevane-Fernandez, M. Aldea, A. G. Garcia, A. Albillos, *J. Neurophysiol.* **2006**, *96*, 1196 – 1202.

[57] R. Pardal, U. Ludewig, J. Garcia-Hirschfeld, J. Lopez-Barneo, *Proc. Natl. Acad. Sci. USA* **2000**, *97*, 2361 – 2366.

[58] E. H. Jaffe, A. Marty, A. Schulte, R. H. Chow, *J. Neurosci.* **1998**, *18*, 3548 – 3553.

[59] a) C. Amatore, S. Arbault, Y. Chen, C. Crozatier, F. Lemaitre, Y. Verchier, *Angew. Chem.* **2006**, *118*, 4104 – 4107; *Angew. Chem. Int. Ed.* **2006**, *45*, 4000 – 4003; b) X. Sun, K. D. Gillis, *Anal. Chem.* **2006**, *78*, 2521 – 2525.

[60] W.-H. Huang, W. Cheng, Z. Zhang, D.-W. Pang, Z.-L. Wang, J.-K. Cheng, D.-F. Cui, *Anal. Chem.* **2004**, *76*, 483 – 488.

[61] P. Chen, B. Xu, N. Tokranova, X. Feng, J. Castracane, K. D. Gillis, *Anal. Chem.* **2003**, *75*, 518 – 524.

[62] a) G. Dernick, L.-W. Gong, L. Tabares, G. Alvarez de Toledo, M. Lindau, *Nat. Methods* **2005**, *2*, 699 – 6708; b) L. Tabares, M. Lindau, G. Alvarez de Toledo, *Biochem. Soc. Trans.* **2003**, *31*, 837 – 841; c) G. Dernick, G. Alvarez de Toledo, M. Lindau, *Nat. Cell Biol.* **2003**, *5*, 358 – 362; d) E. V. Mosharov, L. W. Gong, B. Khanna, D. Sulzer, M. Lindau, *J. Neurosci.* **2003**, *23*, 5835 – 5845; e) A. Albillos, G. Dernick, H. Horstmann, W. Almers, G. Alvarez de Toledo, M. Lindau, *Nature* **1997**, *389*, 509 – 512.

[63] T. Yasukawa, I. Uchida, T. Matsue, *Biophys. J.* **1999**, *76*, 1129 – 1135.

[64] a) C. Amatore, S. Arbault, C. Bouton, K. Coffi, J. C. Drapier, H. Ghandour, Y. Tong, *ChemBioChem* **2006**, *7*, 653 – 661; b) B. A. Patel, M. Arundell, K. H. Parker, M. S. Yeoman, D. O'Hare, *Anal. Chem.* **2006**, 78, 7643 – 7648; c) S. Kasai, H. Shiku, Y.-S. Torisawa, H. Noda, J. Yoshitake, T. Shiraishi, T. Yasukawa, T. Watanabe, T. Matsue, T. Yoshimura, *Anal. Chim. Acta* **2005**, *549*, 14 – 19; d) L. A. Blatter, Z. Taha, S. Mesaros, P. S. Shaklock, W. G. Gier, T. Malinski, *Cir. Res.* **1995**, *76*, 922 – 924.

[65] H. Lu, M. Gratzl, *Anal. Chem.* **1999**, *71*, 2821 – 2830.

[66] A. Devadoss, J. D. Burgess, *J. Am. Chem. Soc.* **2004**, *126*, 10214 – 10215.

[67] *Scanning Electrochemical Microscopy* (Eds.: A. J. Bard, M. V. Mirkin), Marcel Dekker, New York, **2001**.

[68] a) G. Wittstock, M. Burchardt, S. E. Pust, Y. Shen, C. Zhao, *Angew. Chem.* **2007**, *119*, 1604 – 1640; *Angew. Chem. Int. Ed.* **2007**, *46*, 1584 – 1617; b) G. Wittstock, *Fresenius J. Anal. Chem.* **2001**, *370*, 303 – 315; c) M. V. Mirkin, B. R. Horrocks, *Anal. Chim. Acta* **2000**, *406*, 119 – 146; d) G. Nagy, L. Nagy, *Fresenius J. Anal. Chem.* **2000**, *36*, 735 – 744; e) A. L. Barker, M. Gonsalves, J. V. MacPherson, C. J. Slevin, P. R. Unwin, *Anal. Chim. Acta* **1999**, *385*, 223 – 240; f) M. V. Mirkin, *Mikrochim. Acta* **1999**, *130*, 127 – 153.

[69] T. Yasukawa, T. Kaya, T. Matsue, *Anal. Chem.* **1999**, *71*, 4637 – 4641.

[70] M. Tsionky, Z. G. Cardon, A. J. Bard, R. B. Jackson, *Plant Physiol.* **1997**, *113*, 895 – 901.

[71] K. B. Holt, A. J. Bard, *Biochemistry* **2005**, *44*, 13214 – 13223.

[72] J. Mauzeroll, A. J. Bard, O. Owhadian, T. J. Monks, *Proc. Natl. Acad. Sci. USA* **2004**, *101*, 17582 – 17587.

[73] J. Mauzeroll, A. J. Bard, *Proc. Natl. Acad. Sci. USA* **2004**, *101*, 7862 – 7867.

[74] Y. Takii, K. Takoh, M. Nishizawa, T. Matsue, *Electrochim. Acta* **2003**, *48*, 3381 – 3385.

[75] J. M. Liebetrau, H. M. Miller, J. E. Baur, S. A. Takacs, V. Anupunpisit, P. A. Garris, D. O. Wipf, *Anal. Chem.* **2003**, *75*, 563 – 571.

[76] a) S. A. Rotenberg, M. V. Mirkin, *J. Mammary Gland Biol. Neoplasia* **2004**, *9*, 375 – 382; b) W. J. Feng, S. A. Rotenberg, M. V. Mirkin, *Anal. Chem.* **2003**, *75*, 4148 – 4154; c) B. Liu, S. A. Rotenberg, M. V. Mirkin, *Proc. Natl. Acad. Sci. USA* **2000**, *97*, 9855 – 9860.

[77] a) S. Isik, M. Etienne, J. Oni, A. Bloechl, S. Reiter, W. Schuhmann, *Anal. Chem.* **2004**, *76*, 6389 – 6394; b) A. Pailleret, J. Oni, S. Reiter, S. Isik, M. Etienne, F. Bedioui, W. Schuhmann, *Electrochem. Commun.* **2003**, *5*, 847 – 852.

[78] a) V. Ryabova, A. Schulte, T. Erichsen, W. Schuhmann, *Analyst* **2005**, *130*, 1245 – 1252; b) N. Diab, J. Oni, W. Schuhmann, *Bioelectrochemistry* **2005**, *66*, 105 – 110; c) B. Ngounou, S. Neugebauer, A. Frodl, S. Reiter, W. Schuhmann, *Electrochim. Acta* **2004**, *49*, 3855 – 3863; d) S. Isik, J. Oni, V. Rjabova, S. Neugebauer, W. Schuhmann, *Microchim. Acta* **2004**, *148*, 59 – 64; e) S. Neugebauer, S. Isik, A. Schulte, W. Schuhmann, *Anal. Lett.* **2003**, *36*, 2005 – 2020.

[79] a) A. Hengstenberg, C. Kranz, W. Schuhmann, *Chem. Eur. J.* **2000**, *6*, 1547 – 1554; b) M. Ludwig, C. Kranz, W. Schuhmann, H. E. Gaub, *Rev. Sci. Instrum.* **1995**, *66*, 2857 – 2860.

[80] B. Ballesteros Katemann, A. Schulte, W. Schuhmann, *Chem. Eur. J.* **2003**, *9*, 2025 – 2033.

[81] a) Y. Takahashi, Y. Hirano, T. Yasukawa, H. Shiku. H. Yamada, T. Matsue, *Langmuir* **2006**, *22*, 10299 – 10306; b) H. Yamada, H. Fukumoto, T. Yokoyama, T. Koike, *Anal. Chem.* **2005**, *77*, 1785 – 1790; c) D. Oyamatsu, Y. Hirano, N. Kanaya, Y. Mase, M. Nishizawa, T. Matsue, *Bioelectrochemistry* **2003**, *60*, 115 – 121;

d) Y. Lee, Z. E. Ding, A. J. Bard, *Anal. Chem.* **2002**, *74*, 3634 – 3643; e) P. J. James, L. F. Garfias-Mesias, P. J. Moyer, W. H. Smyrl, *J. Electrochem. Soc.* **1998**, *145*, L64 – L66.

[82] a) R. T. Kurulugama, D. O. Wipf, S. A. Takacs, S. Pongmayteegul, P. A. Garris, J. E. Baur, *Anal. Chem.* **2005**, *77*, 1111 – 1117; b) D. O. Wipf, A. J. Bard, D. E. Tallman, *Anal. Chem.* **1993**, *65*, 1373 – 1377.

[83] a) E. N. Ervin, H. S. White, L. A. Baker, C. R. Martin, *Anal. Chem.* **2006**, *78*, 6535 – 6541; b) M. A. Aviles, D. O. Wipf, *Anal. Chem.* **2001**, *73*, 4873 – 4881.

[84] a) R. J. Fasching, S. J. Bai, T. Fabian, F. B. Prinz, *Microelectron. Eng.* **2006**, *83*, 1638 – 1641; b) C. Kranz, G. Friedbacher, B. Mizaikoff, A. Lugstein, J. Smoliner, E. Bertagnolli, *Anal. Chem.* **2001**, *73*, 2491 – 2500; c) J. V. Macpherson, P. R. Unwin, *Anal. Chem.* **2001**, *73*, 550 – 557.

[85] L. Pitta Bauermann, W. Schuhmann, A. Schulte, *Phys. Chem. Chem. Phys.* **2004**, *6*, 4003 – 4008.

[86] A. Schulte, W. Schuhmann in *Electrochemical Methods for* Neuroscience, *Frontiers in Neuroengineering Series*, *Vol. 1* (Eds.: A. Michael, L. M. Borland), Taylor & Francis, Boca Raton, **2006**, chap. 17.

[87] S. Isik, W. Schuhmann, *Angew. Chem.* **2006**, *118*, 7611 – 7614; *Angew. Chem. Int. Ed.* **2006**, *45*, 7451 – 7454.

